ResearchGate

See discussions, stats, and author profiles for this publication at: https://www.researchgate.net/publication/358087856

Hybridization of soft-computing algorithms with neural network for prediction obstructive sleep apnea using biomedical sensor measurements

Article *in* Neural Computing and Applications · June 2022

DOI: 10.1007/s00521-022-06919-w

CITATIONS
2

READS
220

6 authors, including:

Mustafa Habeeb Chyad

2 PUBLICATIONS **6** CITATIONS

SEE PROFILE

Sadik Kamel Gharghan

Middle Technical University

107 PUBLICATIONS **2,113** CITATIONS

SEE PROFILE

Haider Qasim Hamood

Al-Nahrain University

24 PUBLICATIONS **23** CITATIONS

SEE PROFILE

Salah L. Zubaidi

Liverpool John Moores University

77 PUBLICATIONS **1,593** CITATIONS

SEE PROFILE

Some of the authors of this publication are also working on these related projects:

Radiological Techniques View project

Multi-path Effect on Direct Sequence – Code Division Multiple Accesses (DS-CDMA) View project

All content following this page was uploaded by Haider Qasim Hamood on 12 April 2022.

The user has requested enhancement of the downloaded file.

Neural Computing and Applications
https://doi.org/10.1007/s00521-022-06919-w

ORIGINAL ARTICLE

Hybridization of soft-computing algorithms with neural network for prediction obstructive sleep apnea using biomedical sensor measurements

Mustafa Habeeb Chyad[1,2] · Sadik Kamel Gharghan[1] · Haider Qasim Hamood[3] · Ahmed Saleh Hameed Altayyar[4] · Salah L. Zubaidi[5] · Hussein Mohammed Ridha[6]

Received: 19 May 2021 / Accepted: 4 January 2022
© The Author(s), under exclusive licence to Springer-Verlag London Ltd., part of Springer Nature 2022

Abstract

Sleep apnea (SA) is a common respiratory disorder, especially among obese people. It is caused by either the relaxation of the upper respiratory tract muscles or the failure of the neural signal to reach the muscles responsible for breathing, both of which interrupt the patient's sleep–wake cycles. The traditional method for diagnosing this disorder, based on polysomnography, is complicated, vexing, expensive, time-consuming, and requires both sleep centers and specialized staff capable of connecting electrodes to the patient's body. This paper proposes an SA prediction system based on merging five soft computing algorithms, specifically, combining the multi-verse optimizer (MVO) with an artificial neural network (ANN) to leverage measurements from heart rate, SpO_2, and chest movement sensors. The most substantial novelty of this research is the hybridization of MVO and ANN (MVO-ANN), which improves the ANN performance by selecting the best learning rate and number of neurons in hidden ANN layers. This enables highly accurate prediction of sleep apnea events. This work's experimental results reveal that the MVO-ANN performs better than other algorithms, with mean absolute errors of 0.042, 0.202, and 0.166 for training, testing, and validation of the ANN. In addition, the SA prediction system achieved an accuracy of 98.67%, a sensitivity of 96.71%, and a specificity of 99.24%. These results provide good evidence that the proposed method can reliably predict respiratory events in people suffering from SA.

Keywords Artificial neural network · Heart rate · Prediction · SpO_2 · Sleep apnea · Soft computing algorithm

✉ Sadik Kamel Gharghan
sadik.gharghan@mtu.edu.iq

Mustafa Habeeb Chyad
mustfa1521995@gmail.com

Haider Qasim Hamood
prof.haider.almosawi@mtu.edu.iq

Ahmed Saleh Hameed Altayyar
Ahmedaltayyar82@gmail.com

Salah L. Zubaidi
salahlafta@uowasit.edu.iq

Hussein Mohammed Ridha
hussain_mhammad@yahoo.com

[1] Middle Technical University, Electrical Engineering Technical College, Baghdad, Iraq

[2] College of Medicine, University of Al-Ameed, Karbala, Iraq

[3] College of Medicine, Al-Nahrain University, Baghdad, Iraq

[4] Karbala Health Department, Imam Husain Medical City, Karbala, Iraq

[5] Department of Civil Engineering, Wasit University, Wasit, Iraq

[6] Department of Electrical and Electronics Engineering, Faculty of Engineering, Universiti Putra Malaysia, 43400 Serdang, Malaysia

Published online: 24 January 2022

Content courtesy of Springer Nature, terms of use apply. Rights reserved.

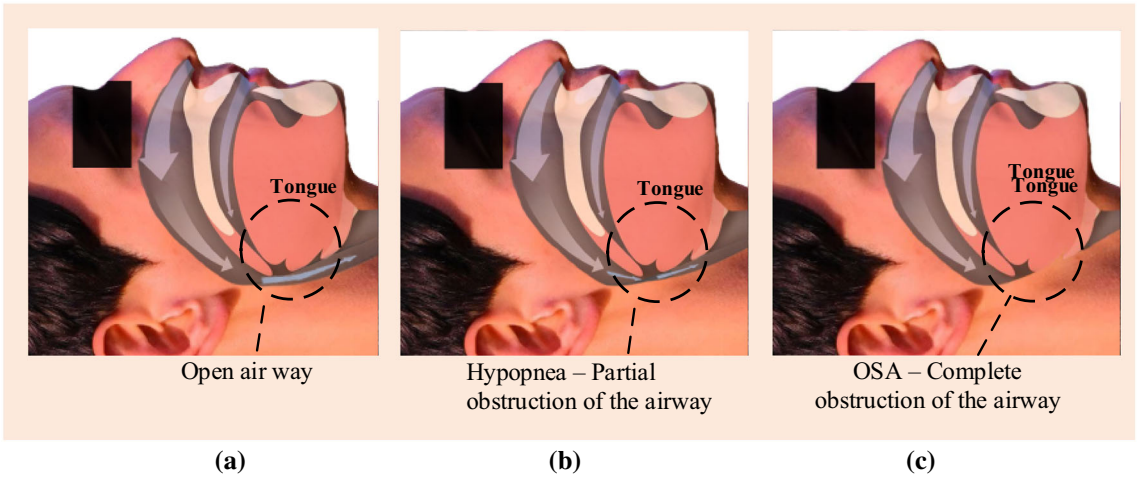

Fig. 1 Upper airway muscles during **a** normal breathing, **b** hypopnea, and **c** obstructive sleep apnea

1 Introduction

Sleep apnea (SA) is among the most prevalent sleeping disorders associated with breathing. It can be described as the repetitive cessation of airflow to the lungs during sleep. A pause of airflow to the lungs that lasts at least 10 s is called a sleep apnea event (SAE), with events accompanied by decreased oxygen saturation in the blood provoking sleep–wake cycles during sleep and fragmenting sleep, preventing patients from getting sufficient sleep. Sleep apnea affects a small proportion (1–2%) of children, a slightly bigger proportion (2–15%) of adults, and more than 20% of seniors, with these numbers constantly increasing [1]. Despite the many consequences associated with SA, the American Academy of Sleep Medicine estimates that 80% of people with the disorder remain undiagnosed [2]. There are three types of SA: obstructive SA (OSA), central SA, and mixed SA. Obstructive SA is caused by the relaxation of the upper airway muscles of the respiratory tract [3], which causes the airway to narrow and prevents the patient from obtaining enough air, as Fig. 1 illustrates. This type is widespread among obese people [4].

Central SA is known as the failure of the neural signal to reach the muscles responsible for breathing [5]. Studies have found that OSA critically induces central SA by invoking breathing instability or narrowing the upper airway. Central SA has also been clinically associated with atrial fibrillation, heart failure, and chronic opioid use [6]. Finally, mixed SA describes a mixture of OSA and central SA factors occurring during a single SAE, that is, an SAE featuring a central pause followed by an obstructive pause.

Symptoms of SA include loud snoring, excessive daytime sleepiness, interrupted breathing events, waking from sleep accompanied by choking or gasping, waking with a dry mouth, waking with a headache, failure to concentrate (potentially causing accidents), night sweating, mood changes (e.g., irritability and depression), and decreased libido. This disorder affects all of the body's organs, ultimately causing or contributing to problems including a weakened immune system, increased heart rate (HR), cardiovascular disease [7], high blood pressure [8], heart attacks, heart failure, type 2 diabetes [9], hormonal changes, enzymatic secretions [10], memory impairment, metabolic problems [11], a sore throat, damaged brain cells [12], certain types of cancer (e.g., lung cancer) [13], reduced life expectancy [10], and, in some cases of OSA, nocturnal death [2]. There are also several eye disorders associated with OSA, namely, floppy eyelid syndrome, optic neuropathy, glaucoma, non-arteritis anterior ischemic optic neuropathy, and papilledema secondary to raised intracranial pressure [14].

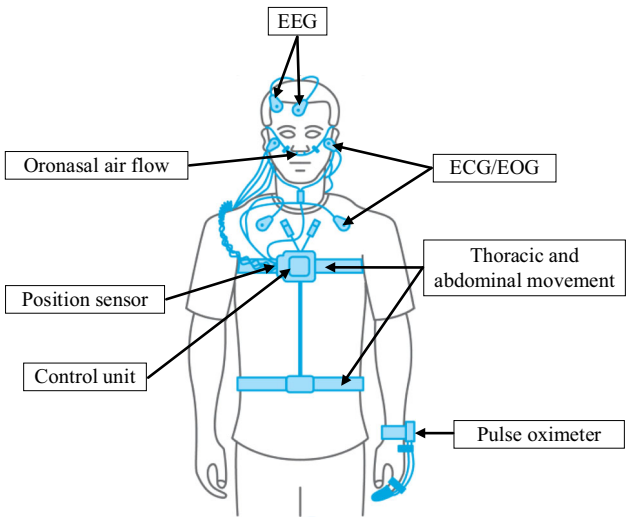

Fig. 2 A graphic representation of the polysomnography test's wire connections

Content courtesy of Springer Nature, terms of use apply. Rights reserved.

There are two main approaches to diagnosing SA. The first method uses polysomnography (PSG) and is the gold-standard method for detecting SAEs [15]; however, PSG is a complicated testing process because it requires various sensors (see Fig. 2) to be attached to the patient's body overnight to collect different bio-signals via electroencephalogram (EEG), electromyogram, electrooculogram (EOG), electrocardiogram (ECG), pulse oximeters, position sensors, nasal airflow sensors [16], and thermistors. Additionally, two auxiliary belts detect chest and abdominal movements [17], and a camera records the patient's sleep. In some countries, people wait several months for the opportunity to be tested using PSG [1], and the average cost of the test can reach $1018 [18]. Besides requiring a sleep laboratory and sleep technicians, PSG is time-consuming and not portable. Given the apparent substantial motivation to address these limitations, we have tried to simplify the method for detecting SAEs and diagnosing SA. The severity of the apnea is measured by an apnea–hypopnea index (AHI), which evaluates the mean number of events occurring in the context of total sleep time.

The second method for SA diagnosis, the home sleep apnea test (HSAT), can be performed at the patient's home and requires fewer sensors than PSG. This test's sensors include a pulse oximeter, nasal airflow sensor, and abdominal and chest belts. The HSAT measures severity level according to a respiratory event index (REI), which measures events in the context of total recording time. Although several trials and studies have tried to simplify the detection of SA, few have focused on predicting SAEs. Several methods have highlighted the utility of the SpO_2 sensor for detecting OSA events [15, 19–23], but the American Academy of Sleep Medicine does not recommend using only this signal for detection [24] because sometimes SAEs occur without any notable change in oxygen saturation. Therefore, methods using SpO_2 must include another sensor to ensure a more reliable model. While some studies have considered the effect of the tracheal sound [25, 26], their approaches preclude collecting sound from overweight people. Several studies have used only EEG, ECG, and EOG signals. However, collecting these signals is a complex process; not only is the processing and feature extraction complicated, but none of them use wireless communication to send the data collected, instead being based on wired connections [12, 23, 27–29], which can irritate patients during the test. Other projects have used imaging systems that require a camera to be positioned in front of a patient's face at a fixed angle [30] or fixed an accelerometer sensor to the patient's chest, although the latter method is only useful for detecting central SA [31]. Elsewhere, the authors of [16] used raw nasal airflow signals with a convolutional neural network (CNN) for detection. However, the invasive sensor renders the test rather uncomfortable. Elsewhere, the authors of [18] tested a combination of SpO_2 and HR sensors with an artificial neural network (ANN).

Although various previous studies have tried to simplify examination methods and use the fewest sensors to diagnose respiratory events, there exist multiple gaps in the literature. For example, many of these previous studies focused on detection, not considering predicting respiratory events before they happen. Additionally, few studies have investigated central SA. In contrast, the current study highlights central SA by employing a flex sensor that is fixed on the patient's chest to detect chest movements stopping and indicate the patient's breathing patterns. Meanwhile, studies that collect ECG, EOG, and EEG signals complicate signal collection because the electrodes connected to different parts of the body do not use wireless techniques to send signals, increasing the number of wires that are connected to a patient's body and making them feel uncomfortable when moving in their sleep. Pre-processing signals further complicates such procedures.

Having considered the limitations of previous studies, this research considers the design and implementation of a small low-cost and high-reliability sleep apnea system (SAS) that combines three sensors (i.e., SpO_2, HR, and flex sensor) with Bluetooth low-energy 4.0 (BLE 4.0) to send recorded data to the monitoring unit (MU). The most substantial novelty of this research is the hybridization of the multi-verse optimizer (MVO) and artificial neural network (ANN) mechanisms as MVO-ANN, an approach that improves the ANN performance by selecting the best learning rate and number of neurons in hidden ANN layers. This enables highly accurate prediction of SAEs. Importantly, an ANN is flexible and can manage a large amount of data without any manual intervention [5, 32]. The accuracy, sensitivity, and specificity of the SAS have been confirmed by a series of statistical analyses that demonstrate that the device achieves data collection accuracy of 99.94% when compared with the benchmark (BM) device (Alice PDx PHILIPS Respironics) [41]. Figure 3 illustrates the research process as a flow chart.

This paper's contributions can be summarized as follows:

1. An easy-to-install, small, and lightweight device was designed and implemented to predict and detect SAEs. Only a few sensors (i.e., HR, SpO2, and flex) were included, reducing stress on the patient because they are only attached to the patient's body in the form of a hand-wearable device. Additionally, the proposed hand-wearable device was demonstrated to be convenient, not hindering patient movement during sleep because it does not use a wired connection, instead

Content courtesy of Springer Nature, terms of use apply. Rights reserved.

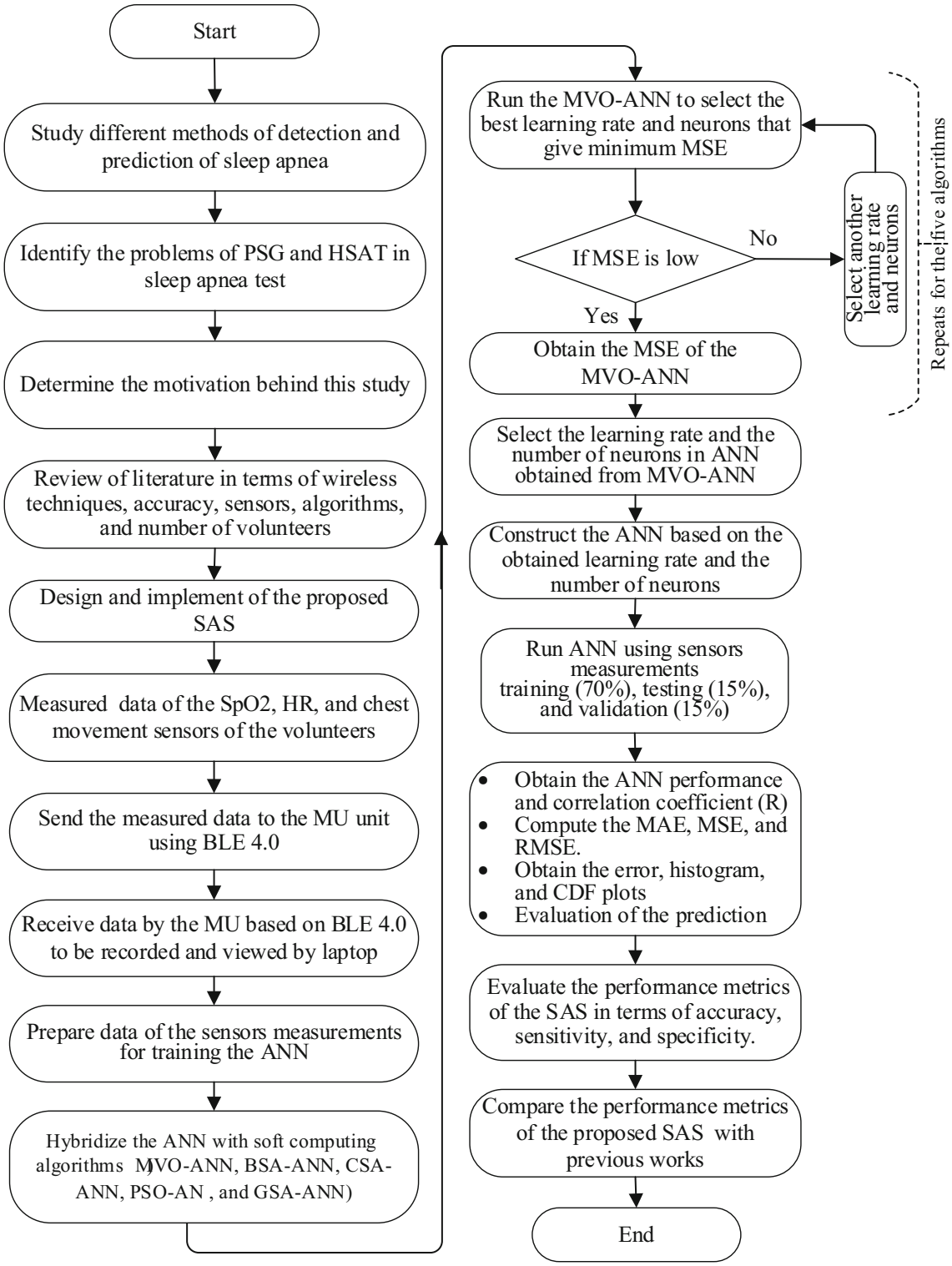

Fig. 3 Flow chart illustrating the research process

transmitting data wirelessly from the patient to the MU over BLE 4.0.

2. Using the ANN technique, SAEs were accurately predicted before they happened, and using the MVO algorithm improved the ANN's performance in terms of learning rate and number of neurons in the ANN's hidden layers.

Content courtesy of Springer Nature, terms of use apply. Rights reserved.

2 Related works

In the past decade, many studies have focused on diagnosing SA, using various vital signals to detect respiratory events. Notably, Erdenebayar et al. [33] proposed methods for automatically detecting SAEs using deep learning approaches, conducting a study dependent on a single ECG lead. The detected signal was pre-processed, normalized, and segmented at 10-s intervals. Six deep learning approaches were designed and implemented to automatically detect SAEs, including deep neural network (DNN), one-dimensional CNN, two-dimensional CNN, recurrent neural networks, long short-term memory (LSTM), and gated recurrent unit (GRU). Data were collected from 86 patients, with 69 included in the training set and 17 included in the test set. The most accurate performance was observed for the gated recurrent unit (99%) and one-dimensional CNN (98.5%). This study also distinguished OSA and hypopnea using ECG signals. However, the study could not recognize other SA types (i.e., central SA and mixed SA), and the ECG signal could be impure due to changes in sleeping position, coughing during sleep, and loud snoring.

Meanwhile, Ferduła et al. [1] developed a method for detecting SAEs that did not require specialist equipment or sleep experts to analyze bio-signals. That study was divided into three stages: recognition of apnea and hypopnea, recognition of sleep stage, and determination of each stage's duration. All of these measurements used a pulse oximeter sensor with ANN, with the data used to train the neural network collected from eight patients. The neural network was trained, validated, and tested using the "Levenberg–Marquardt (LM)" algorithm from the MATLAB Neural Network Toolbox with 32 input neurons and 10 hidden layers. However, that study did not consider other SA types or report SAE detection accuracy. Elsewhere, the authors of [34] proposed a method for estimating SA severity level by adopting deep learning algorithms. Their model comprised an accelerometer fixed over a suprasternal notch that detected respiratory movements, and they collected data from 69 participants during PSG. Twenty-one features were extracted from the accelerometer signal to classify deep learning, detect SAEs, and determine AHI. The authors combined CNN with an LSTM layer and a fully connected layer to create a classifier for measuring AHI, with the output's performance assessment indicating 81% sensitivity, 87% specificity, and 84% accuracy. Certain limitations were acknowledged; for example, the AHI was estimated according to total recording time, and the classifier could not recognize event type.

The authors of [35] described a method for detecting SAEs based on EEG signals, conducting a study using only CNN to extract features of the EEG signals to determine apnea or non-apnea events with DNN. The method was trained and tested on 25 patients, with the results suggesting that the approach could detect events using online data collection. However, this method only detected normal breathing and respiratory events, precluding estimation of all event types. Additionally, the EEG signal is considerably complex to process. Elsewhere, Sankar et al. [36] suggested a method for detecting SAEs involving adopting respiratory signals using a supervised neural network. The output is classified into normal respiration, apnea events, and motion artifices. Five different backpropagation algorithms for training were adopted, including LM, scaled conjugate gradient, the Broyden–Fletcher–Goldfarb–Shanno algorithm, one step secant, and Powell–Beale restarts for classifying the three outputs. Respiratory data were collected from the MIT-BIH database and included 1,200 data points. The best performance was observed for LM algorithms with 4 input neurons, 20 hidden layers, 3 output neurons, and a maximum of 100 epochs, with accuracy reaching 98.7%. One limitation was the inconvenience of collecting respiratory signals due to the sensor locations.

Meanwhile, the authors of [37] suggested a method using an EEG signal and three different classifiers for apnea detection. The EEG signal was pre-processed with the Infinite Impulse Response bandpass filter and the Hilbert Huang Transform for smoothing and sub-band division of the signals. Next, the signal was analyzed by the support vector machine (SVM), *K*-nearest neighbors, and ANN to determine apnea events. Data from 18 patients were collected from the MIT-BIH database to train, test, and measure the performance. The best accuracy was observed for the SVM (99%). However, the study was limited by the complexity of the EEG signal analysis and the demand for signal recording for several electrodes on the scalp. Elsewhere, Wang et al. [38] proposed a method for detecting apnea events using a single ECG lead. To detect SAEs, they adopted five algorithms: linear discriminant analysis, SVM, logistic regression, non-time-window multilayer perceptron (MLP), and time window MLP (TW-MLP). The researchers focused on TW-MLP with one hidden layer, using the FIR filter and the Hamilton algorithm for feature extraction. The data were collected from the PhysioNet database, and the TW-MLP algorithm demonstrated the best performance: 87.3% accuracy, 85.1% sensitivity, and 88.7% specificity. However, this approach could not differentiate between apnea and hypopnea.

The authors of [39] proposed a novel approach to detecting respiratory events that involved using a wearable device that connected around the neck or was attached to

Content courtesy of Springer Nature, terms of use apply. Rights reserved.

the chest using adhesive tape. The device recorded various signals: chest bio-impedance, ECG (two leads), and patient motion (using an accelerometer). The algorithm implemented to automatically detect SAEs was LSTM. Data from 25 participants were collected for the training network. Although the device's performance was sub-optimal (58.4% sensitivity, 76.2% specificity, and 72.8% accuracy), this study included all three types of SA. However, several sensors were needed to use the wearable device, which could be tedious for the patient. The authors of [40] presented a method for detecting SAEs among infants that implemented FPGA. The system combined two sensors: polyvinylidene fluoride for breathing and a pulse oximeter for measuring oxygen saturation. The proposed method implemented the Feedforward network as a classifier with five hidden layers, and the network output used "1" to denote apnea and "0" to indicate normal breathing. The data for the training network was derived from the PhysioNet database, and the classifier surpassed 85% accuracy.

Finally, the authors of [41] described a method for detecting SAEs that depended on deep learning approaches, combining CNN and LSTM. They used the ECG signal as input after measuring the signal's RR interval. Data from 35 patient recordings of ECG signals (from the PhysioNet database) were used to train and test the method, and the classifier recognized the presence or absence of SAEs, reaching 96.94% specificity, 98.97% sensitivity, and 99.80% accuracy.

After reviewing the limitations of these previous studies, the current research project involved developing solutions to address these shortcomings, which has involved designing and implementing a small hand-worn device that is affordable and portable. By reducing the number of sensors connected to the patient's body by using only two parts—namely, the pulse oximeter, which measures HR and SpO_2, and the flex sensor, which is attached to the patient's chest with medical plaster tape to measure the chest movement—this SAS reduces the amount of stress on the patient during the examination period. Finally, the SAS uses BLE 4.0 to send the data collected to the MU, where artificial intelligence techniques are used to recognize and predict respiratory events.

3 Development of the proposed system

Studying previous works to find solutions to complications associated with diagnosing SA and encountering the limitations of existing approaches motivated this project. Accordingly, this research's SAS works to predict respiratory events before they occur and is characterized by its small size and combination of three sensors. Additionally, it is hand-worn and utilizes BLE 4.0, enabling it to send the data measured from the patient's body to the MU. The schematic diagram of the SAS includes the transmitter unit and MU (see Fig. 4). The transmitter unit comprises a pulse oximeter sensor (MAX 30,101) that can measure SpO_2 and HR, a flex sensor, an Arduino Nano microcontroller based on the Atmega 328p chip, and BLE 4.0 (HM-10 model), which sends the recorded data from the sensors to the MU, as Fig. 4a shows. The transmitter unit is powered by a lithium-ion battery (3.7 V/4000 mAh) that can support 17 h of continuous monitoring, which can adequately monitor the participant for seven hours of sleep. Meanwhile, the MU comprises BLE 4.0, an Arduino UNO microcontroller based on the Atmega 328p chip, and a laptop, as Fig. 4b shows. Figure 4c depicts the transmitter device. Because the laptop powers the components of the MU (i.e., BLE 4.0 and Arduino UNO), it requires no battery source. The laptop also enables the MU to utilize ANN techniques. Table 1 presents the specifications of the sensors and hardware adopted by the transmitter and the MU, with the results obtained from the SAS compared with those of other approaches to confirm the SAS's performance.

4 Experimental configuration

The data were collected from 10 participants over the course of seven hours of sleep per participant, six of whom suffered from SA, and four of whom were healthy. A total of 252,000 samples (84,000 samples from each of the three sensors, i.e., HR, SpO_2, and flex) were collected, meaning 25,200 samples (8400 samples from each of the three sensors) were collected from each participant. The HR, SpO_2, and flex for each participant were sampled at a frequency of 1 Hz. This frequency was selected because (i) several previous works have adopted it, following [42–44], (ii) the HSAT device measures the parameters with a sampling frequency of 1 Hz, enabling fair comparisons of the performance metrics with HSAT, and, (iii) although an ideal sample frequency has yet to be established [44], Nigro et al. [45] observed that a minimum data sampling rate of 0.25 Hz can adequately avoid loss of oximetry resolution through sleep tests. However, we considered a sampling frequency four times greater than that suggested by [45]. Therefore, adopting a sampling frequency of 1 Hz to collect data from the three sensors did not influence the performance of the proposed SAS during the sleep test.

The conditions for compliance with the standards of ethical conduct of the Helsinki Declaration were met (Finland 1964), with written informed consent acquired before beginning the experiment after a thorough explanation of the research to the volunteer. Searching for these

Content courtesy of Springer Nature, terms of use apply. Rights reserved.

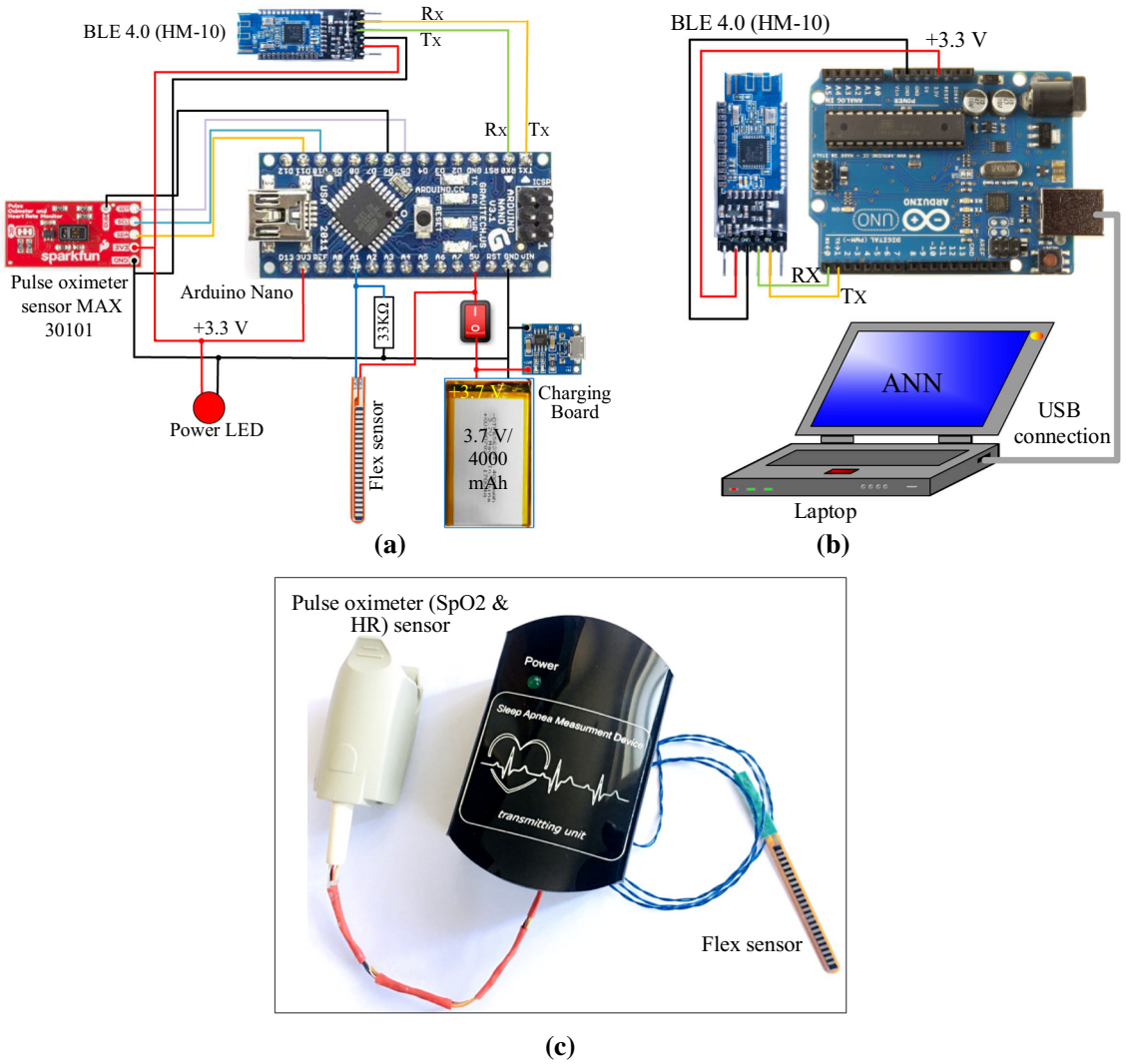

Fig. 4 Schematic diagrams of **a** the sleep apnea system's transmitter unit and **b** the sleep apnea system's monitoring unit, and **c** a snapshot of the sleep apnea system's transmitter unit

subjects took approximately four months. Despite the numerous people suffering from SA, 80% of those affected do not receive a diagnosis. This is partly due to the limited number of patients with scientific knowledge of sleep testing, limited sleep center availability, the high costs of sleep centers, and certain doctors not having sufficient experience to address such pathologies. The current research selected six patients (out of 10 participants) with respiratory disorders, who were examined and diagnosed to suffer from obesity, with substantial fatty tissue around the neck, nighttime bottlenecks, and loud snoring. Additionally, they ranged in age from 50 to 53 years and suffered from chronic diseases, including hypertension.

These participants were examined using an HSAT device comprising a pulse oximeter, nasal airflow sensor, thermistor, and two belts to measure breathing effort (one around the abdomen and another around the chest). Installing the HSAT device on the patient took between 15 and 20 min. In contrast, it took about 3–5 min to attach the developed SAS and configure the MU. The six volunteers with SA recorded average REIs of around 60 events per hour, potentially indicating severe levels of SA.

Upon linking the testing devices to the patient's body, the SAS and the BM device (i.e., HSAT) recorded measurements at the same time after finishing connecting the two devices. The BM device recorded chest and abdominal movement, HR, SpO_2, and airflow through the nose and mouth; these data were recorded on an SD card to be analyzed later by the doctor to determine the frequency of SAEs. The SAS data measured SpO_2, HR, and chest movement. The measured data were sent to the MU via BLE 4.0. The MU's laptop utilized ANN procedures to predict respiratory events.

Content courtesy of Springer Nature, terms of use apply. Rights reserved.

Table 1 The specifications of the sensors and hardware adopted by the transmitter unit and the monitoring unit

Sensor/hardware	Description
Pulse oximeter sensor MAX 30,101	HR monitor and pulse oximeter sensor
	LEDs present (Green, Red, Infrared)
	Typical supply voltage: + 3.3 V
	Current consumption: 0.6 mA
Flex sensor	Typical supply voltage = + 3.7 V
	Current consumption: 135 mA @ 3.7 V
	Resistance in normal position (flat): 25 KΩ
	Bend resistance: 45–125 KΩ
Bluetooth low-energy 4.0	Model: BLE 4.0 (HM-10)
	Working voltage: + 3.3 V
	Current consumption: 50 mA
	Communication range: 100 m
	Frequency: 2.4 GHz ISM band
Arduino Nano	Working voltage: + 5 V can operate on + 3.3 V
	Current consumption: 19 mA
	Clock speed: 16 MHz
Power LED	Red LED 3 mm
	Working voltage: + 2– + 2.2 V
	Current consumption: 20 mA
Transmitter unit battery	Lithium-ion battery (3.7 V/4,000 mAh)
Arduino UNO	Working voltage: + 5 V can operate on + 3.3 V
	Current consumption: 50 mA
	Clock speed: 16 MHz
Laptop	Monitors the sensor measurements
	Executes MVO-ANN procedures
	Computer type: HPF7AKP
	Processor: Intel (R) Core (TM) i7-7500U CPU@ 2.70 GHz 2.90 GHz
	System type: 64-bits operating system
	RAM: 16 GB
	Operating system: Window 10 Pro
	Software versions:
	MATLAB R2015b
	Arduino IDE 1.8.7

Total current consumption of the transmitter unit = 0.6 + 135 + 50 + 19 + 20 = 224.6 mA

Battery capacity = 4000 mAh

Battery lifetime = (4000/224.6) = 17 h

The first SA patient produced an average REI of 56 events per hour, which included 52 SAEs and 4 hypopnea events, with the maximum duration for apnea reaching 90 s and the average SAE lasting approximately 39 s. The lowest level of oxygen observed in the blood was 70%.

The second SA patient experienced more severe interruptions than the first, recording an average REI of 70 events per hour. However, the nature of the respiratory events most likely indicated hypopnea; 40 events characterize hypopnea, and hypopnea events can reach 60 s (apnea events only reach 35 s). The minimum level of oxygen in the blood during sleep was 78%. Figure 5a shows the second patient preparing for the examination.

The third SA patient, who also suffered from severe respiratory interruptions, recorded an average REI of 65 events per hour, with 35 events indicative of hypopnea and the other 30 indicative of apnea. The maximum duration of events was 52 s for apnea and 97 s for hypopnea. Figure 5b shows the third patient during the connection of the HSAT and the SAS. Notably, these six participants had

Content courtesy of Springer Nature, terms of use apply. Rights reserved.

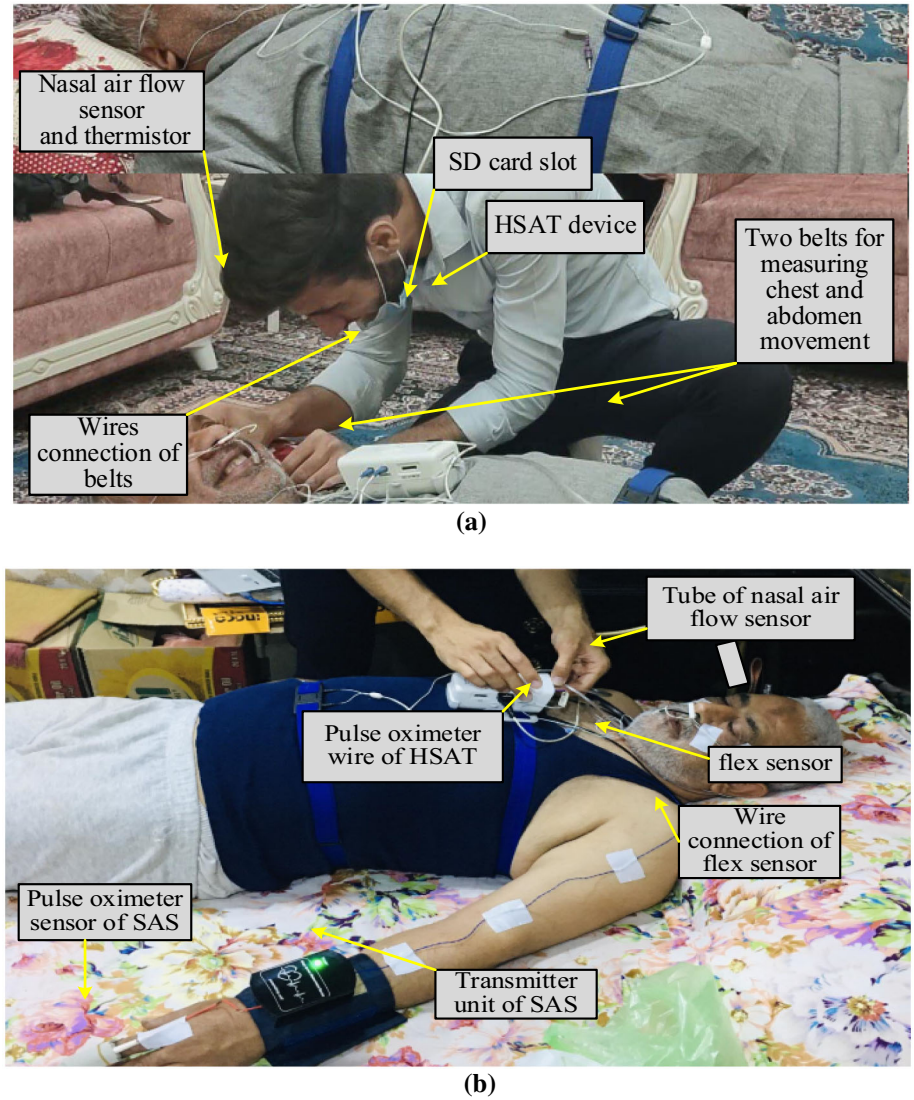

Fig. 5 Experiment preparation: **a** patient while preparing for the examination and **b** connection of the home sleep apnea test and the developed sleep apnea system to the patient

already been diagnosed with SA and needed positive airway pressure devices to achieve adequate sleeping time and rest during sleep. Meanwhile, the four healthy participants (ranging in age between 18 and 27 years) did not suffer from any SA symptoms, recording levels of oxygen in the blood exceeding 96%.

5 Data collection

Data were collected from the 10 participants, and the data were divided into training (70%), test (15%), and validation of the ANN (15%). As mentioned, a total of 252,000 data points were collected for the 10 participants (25,200 for each participant) using the SAS. To ensure the device's validity, these data were compared with the BM device by conducting a set of statistical analyses. Figure 6a (first experiment), Fig. 6b (second experiment), Fig. 6c (third experiment), and Fig. 6d (fourth experiment) compare the oxygen saturation of four persons suffering from SA with that of the healthy volunteers. This information represents a period of approximately 10 min, during which there were 13 consecutive SAEs.

Figure 7a (first experiment), Fig. 7b (second experiment), Fig. 7c (third experiment), and Fig. 7d (fourth experiment) compare the HR variability between the four patients suffering from SA and the four healthy volunteers; again, this information represents a period of only ten minutes, with the figures making clear that the HR of the SA patient is consistently higher than that of the healthy subject. People with SA demonstrate higher HRs than normal persons due to the effectiveness of the parasympathetic system, which seeks to compensate for the lack of oxygen in the blood by increasing blood flow [46].

The flex sensor records chest movements after the sensor is attached to the chest, with this flex sensor recording

Content courtesy of Springer Nature, terms of use apply. Rights reserved.

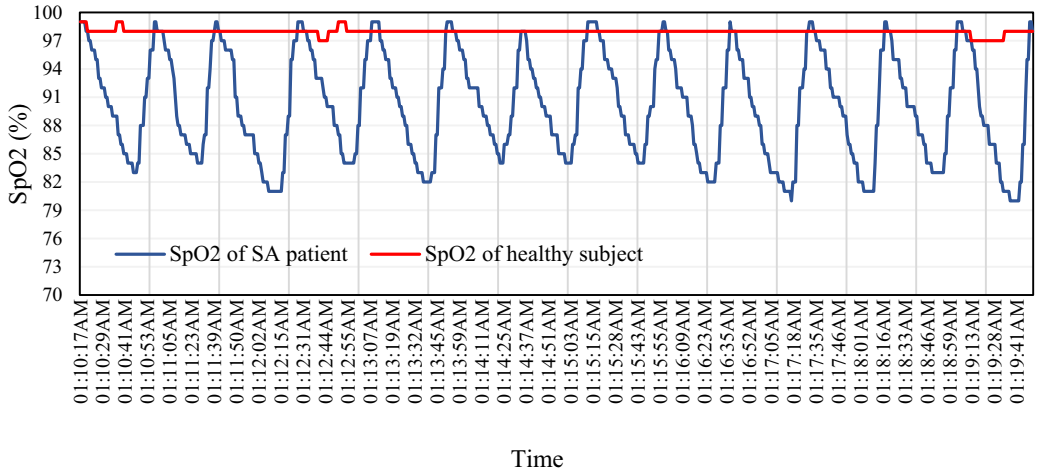

(a)

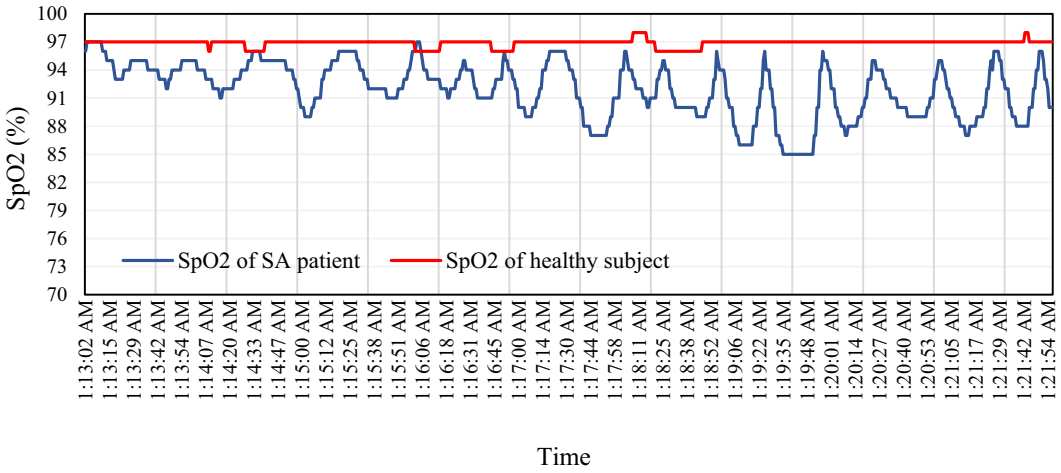

(b)

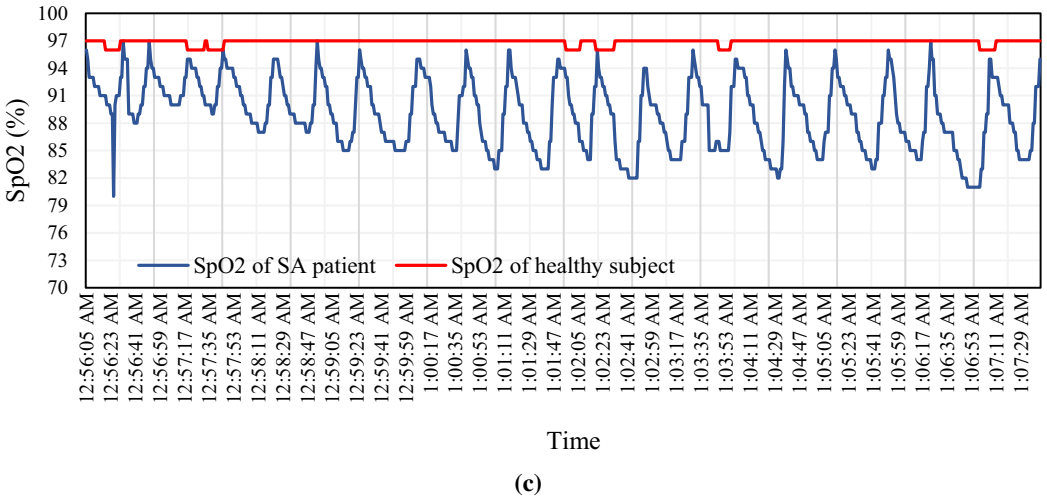

(c)

Fig. 6 Comparing the oxygen saturation between a healthy participant and a sleep apnea patient: **a** first experiment, **b** second experiment, **c** third experiment, and **d** fourth experiment

Content courtesy of Springer Nature, terms of use apply. Rights reserved.

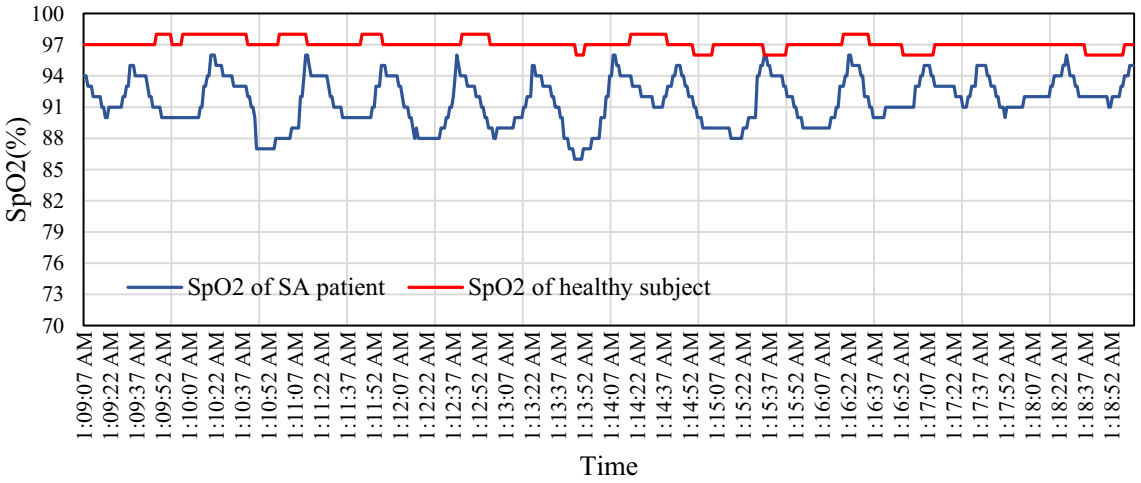

(d)

Fig. 6 continued

the chest's rise and fall, representing the movement that results from the breathing process, an oscillatory movement that is depicted in Fig. 8a (first experiment), Fig. 8b (second experiment), Fig. 8c (third experiment), and Fig. 8d (fourth experiment). The figures show certain peaks, which reflect either the patient's movement during sleep—meaning fluctuations of sleep—or deep breathing, which produces amplified readings that are recorded in the form of peaks.

6 Artificial neural network hybridized with soft-computing algorithms

This research adopted an ANN to predict patient SAEs. The measured data (i.e., the biomedical parameters HR, SpO_2, and chest movement) were split into three groups: training, validation, and testing. A total of 252,000 samples were recorded, representing 84,000 samples for each of the three parameters. This means that 8400 samples for each of the three parameters were collected from each participant. For each parameter, 70% (5880 of 8400) of samples were used for training, 15% (1260 of 8400) were used for testing, and 15% (1260 of 8400) were used for validation. Choosing these three parameters and the percentages of the measured samples allocated to the different sets follows the approach adopted by many earlier articles, e.g., [47–49]. The number of neurons in the hidden layer and the ANN learning rate were key factors in designing the ANN architecture. Although several earlier researchers adopted a trial-and-error method to select these key factors [50–55], this trial-and-error method is not always secure, featuring considerable computational complexity and being prone to errors [56]. Additionally, the trial-and-error method can lead to a large number of neurons in the hidden layer, potentially overfitting the data [57]. Thus, the method cannot be considered an optimal solution, and an effective soft-computing algorithm should be hybridized with an ANN to select the learning rate and number of neurons in the ANN's hidden layers.

Choosing an efficient algorithm is not an easy task and poses another challenge, requiring various soft-computing algorithms—namely, Particle Swarm Optimization (PSO), Gravitational Search Algorithm (GSA), Backtracking Search Algorithm (BSA), Crow Search Algorithm (CSA), and MVO—were hybridized with the ANN to choose the one that provided a fast convergence and a low minimum mean square error (MSE) with minimal iterations. The optimization algorithms are sets of processes that iteratively compare several solutions until arriving at an optimal or suitable solution. The algorithms were executed for 40 swarms and 100 iterations, with 40 swarms chosen because, according to [58], it provides an appropriate MSE. The MVO-ANN algorithm (Fig. 9) was observed to produce a lower MSE than the other algorithms during the training process (see Fig. 10). The number of neurons in each hidden layer (see Table 2) was obtained automatically after the training process for each soft-computing algorithm without any manual intervention. Additionally, the MVO-ANN featured faster convergence than the other soft-computing algorithms, reaching the minimum error after 28 iterations. In contrast, the BSA-ANN recorded the highest MSE of the five algorithms. Table 2 presents the learning rate, the number of neurons in the first and second

Content courtesy of Springer Nature, terms of use apply. Rights reserved.

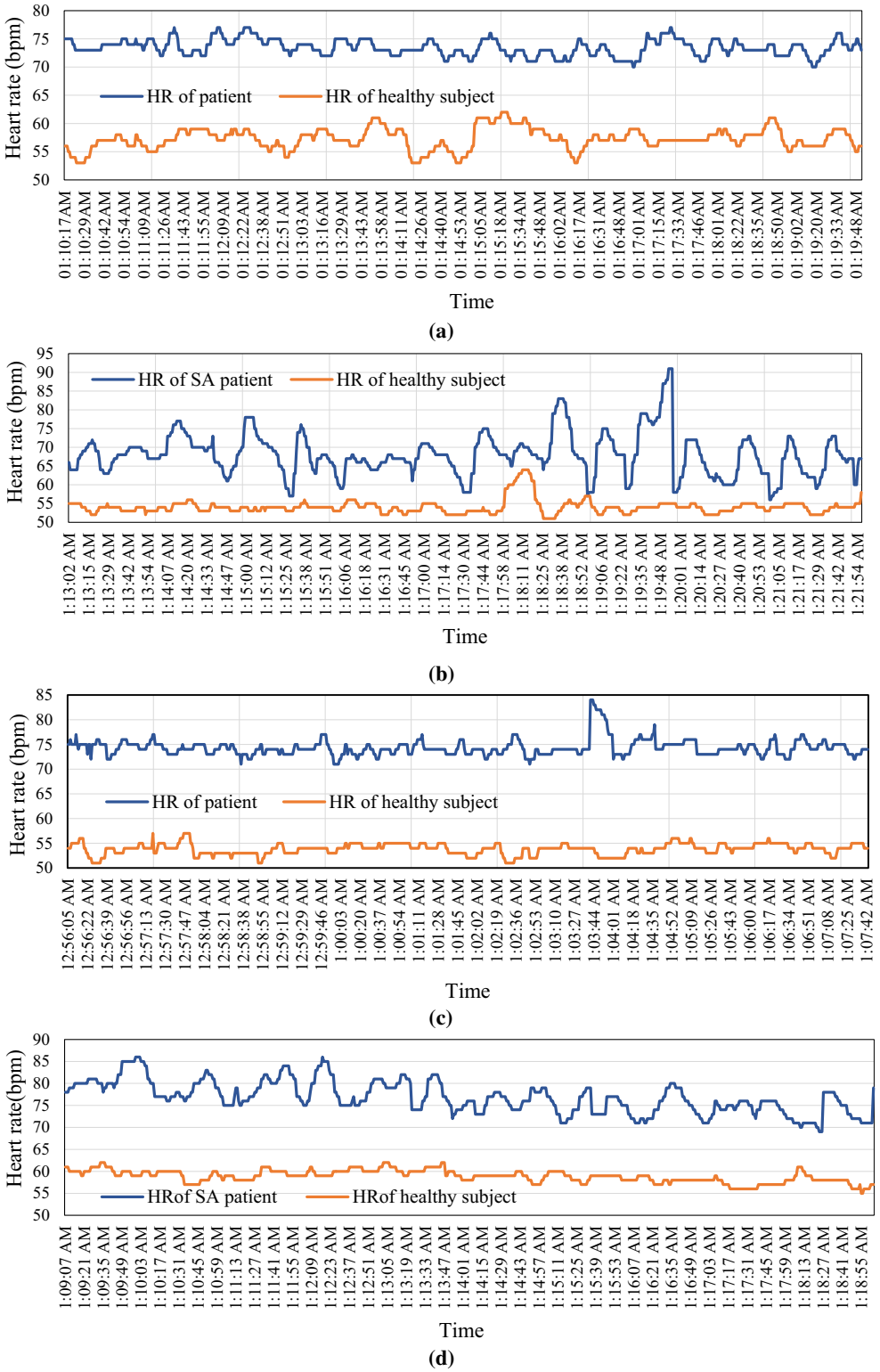

Fig. 7 Comparing the heart rate variability between a healthy participant and a sleep apnea patient: **a** first experiment, **b** second experiment, **c** third experiment, and **d** fourth experiment

Content courtesy of Springer Nature, terms of use apply. Rights reserved.

hidden layer of the ANN, and the MSE at a specific iteration for each of the five algorithms.

The mathematical formulae for the MVO algorithm were presented in [59] and are reproduced as Eq. (1) through Eq. (5). The equations were followed to obtain the optimal number of neurons in the first and second hidden layers and obtain a learning rate capable of achieving the MSE.

$$\vartheta_i^j = \begin{cases} \vartheta_k^j & ran1 < NOR(u_i) \\ \vartheta_i^j & ran2 \geq NOR(u_i) \end{cases} \tag{1}$$

where ϑ_k^j represents the jth factor of kth universe chosen by a roulette wheel selection mechanism, ϑ_i^j represents the jth factor of ith universe, *ran1* and *ran2* are the random numbers that are disseminated between 0 and 1, and $NOR(u_i)$ is the normalized inflation rate of the ith universe, which ith universe (u_i) can be formulated according to Eq. (2).

$$u_i = \begin{bmatrix} \vartheta_1^1 & \vartheta_1^2 \ldots\ldots \vartheta_1^p \\ \vartheta_2^1 & \vartheta_2^2 \ldots\ldots \vartheta_2^p \\ \cdot & \cdot \\ \cdot & \cdot \\ \cdot & \cdot \\ \vartheta_n^1 & \vartheta_n^2 \ldots\ldots \vartheta_n^p \end{bmatrix} \tag{2}$$

where n is the number of candidate universes and p is the number of parameters.

$$\vartheta_i^j = \begin{cases} \begin{cases} Y_j + TR \times \left((UR_j - LR_j) \times ran4 + lo_j \right) & ran3 < 0.5 \\ Y_j - TR \times \left((UR_j - LR_j) \times ran4 + lo_j \right) & ran3 \geq 0.5 \end{cases} & ran2 < WP \\ \vartheta_i^j & ran2 \geq WP \end{cases} \tag{3}$$

where Y_j denotes the *jth* boundary of the best universe framed up until this point, *TR* is the coefficient that denotes the traveling distance rate, *WP* is the coefficient that indicates the wormhole existence probability, LR_j and UR_j are the lower and upper bounds of the jth variable, and *ran2*, *ran3*, and *ran4* are the random numbers that are scattered between 0 and 1.

The *WP* and *TR* can be calculated using Eqs. (4) and (5):

$$WP = \left(\frac{\text{maximum} - \text{minimum}}{t} \right) \times \tau + \text{minimum} \tag{4}$$

$$TR = 1 - \frac{\tau^{1/\beta}}{t^{1/\beta}} \tag{5}$$

where the values of maximum and minimum of the wormhole existence probability in Eq. (4) were adopted as 1 and 0.2 in the current work. These values were selected following the recommendations of [59–62].

Meanwhile, τ and t represent the present and maximum iterations (100 maximum iterations and 1 present iteration implemented in this paper). In Eq. (5), the parameter β is the exploitation precision over the iterations, which equals 6 in the current research. The larger the value of this parameter (i.e., β), the quicker and more accurate the local search will be.

The MVO-ANN algorithm (Fig. 9) proved capable of producing an MSE of 0.11 at 28 iterations, as Fig. 10 shows, meaning that the performance of an ANN can be improved in terms of computational complexity and MSE, allowing the ANN to successfully predict SA. The MVO-ANN algorithm was consequently used for the current research, with the number of neurons in the first hidden layer equaling 20, the number in the second hidden layer equaling 18, and the learning rate recorded as 0.751 (see Table 2). These values could be used in the ANN, and the ANN could be run until reaching the MSE between the actual and predicted SAE.

7 Artificial neural network structure

After determining the numbers of neurons in the first and second hidden layers and the learning rate, the ANN architecture could be designed, as Fig. 11 shows. The parameters of the ANN are listed in Table 3, with the network's output denoted by "0", which describes normal or healthy breathing, "1", which denotes hypopnea, and "2", which indicates apnea.

8 Results and discussions

This section presents the results concerning the measurement accuracy of the proposed SAS relative to the BM device and the ANN's capacity to predict respiratory events. These results emphasize the results obtained from the MVO-ANN algorithm because it performed better than the other methods (i.e., GSA-ANN, BSA-ANN, CSA-ANN, and PSO-ANN) in terms of MSE. As shown in Fig. 9, the MSE of MVO-ANN reached 0.11, the lowest among these networks. The results presented in this section are divided into three parts.

8.1 Measurements accuracy results

To validate the performance of the proposed SAS, the HR and SpO_2 measurements obtained from both the proposed SAS and the BM device were investigated for accuracy. Accuracy was measured according to Eq. (6), and the accuracy of the proposed SAS—compared against the BM device—was observed to reach 99.94%. This high accuracy suggests that the HR and SpO_2 measurements recorded by the proposed SAS were comparable to the measurements recorded by the BM device.

Content courtesy of Springer Nature, terms of use apply. Rights reserved.

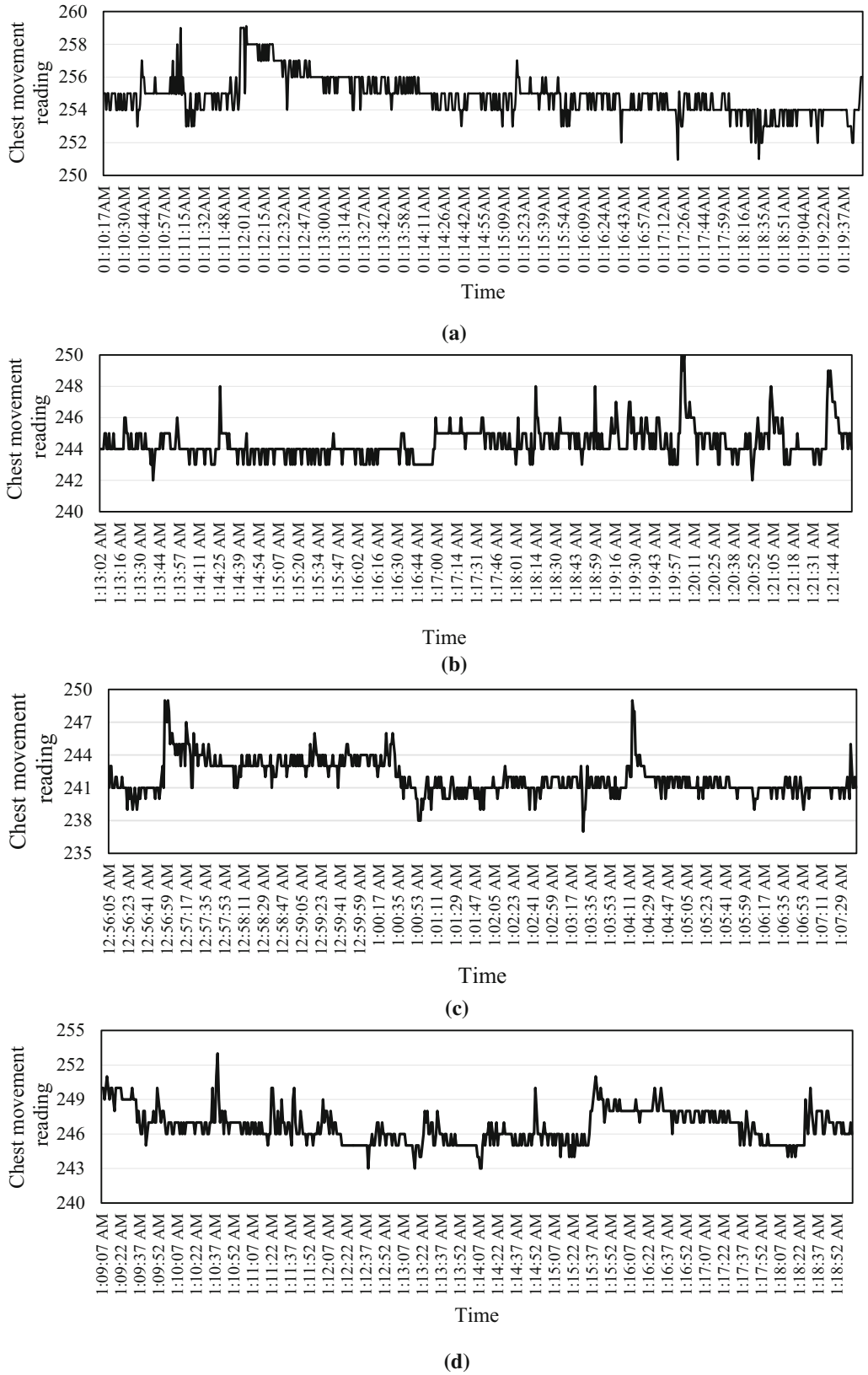

Fig. 8 Chest movements obtained from a flex sensor: **a** first experiment, **b** second experiment, **c** third experiment, and **d** fourth experiment

Content courtesy of Springer Nature, terms of use apply. Rights reserved.

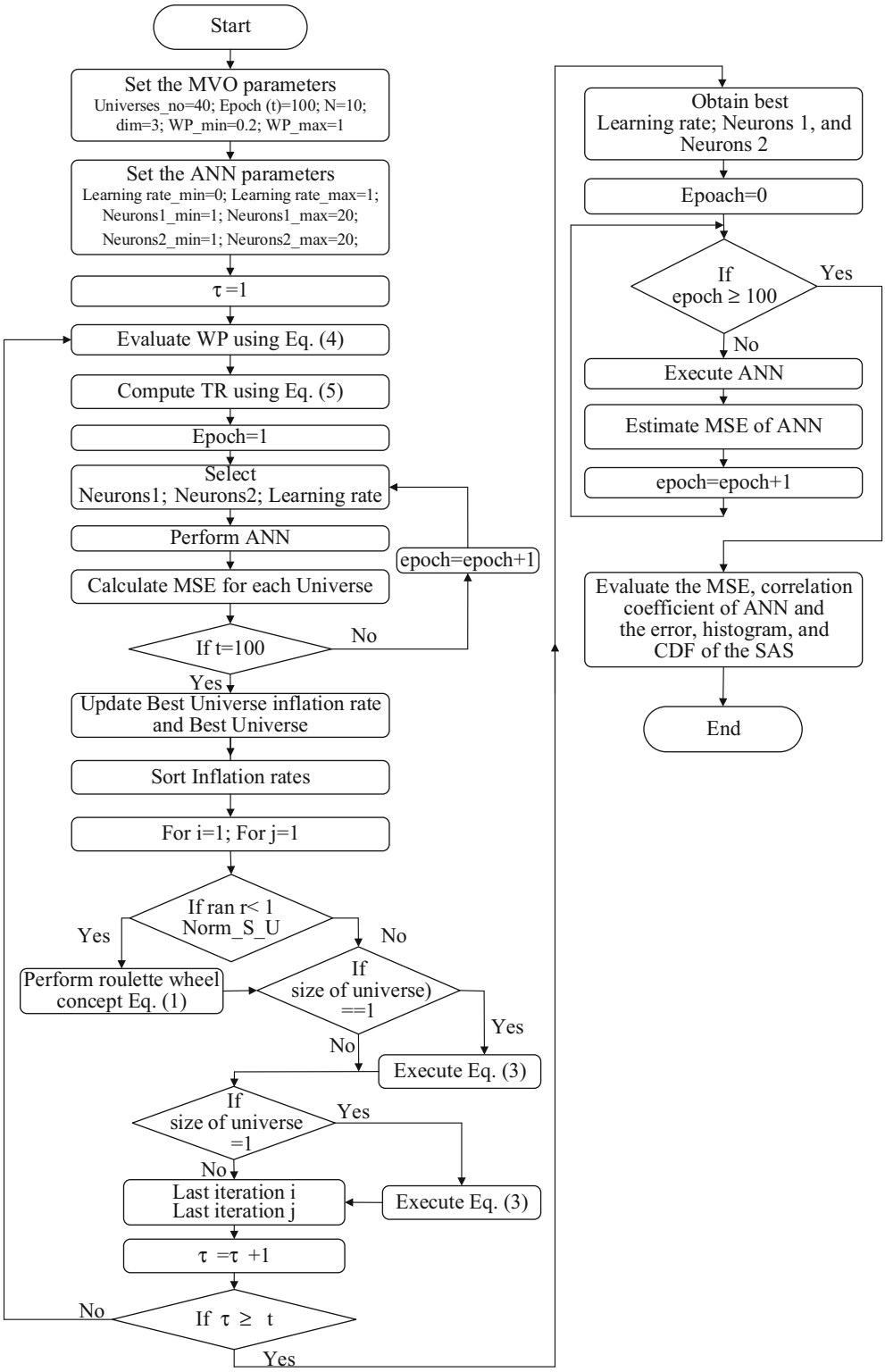

Fig. 9 The multi-verse-optimizer–artificial-neural-network algorithm

Content courtesy of Springer Nature, terms of use apply. Rights reserved.

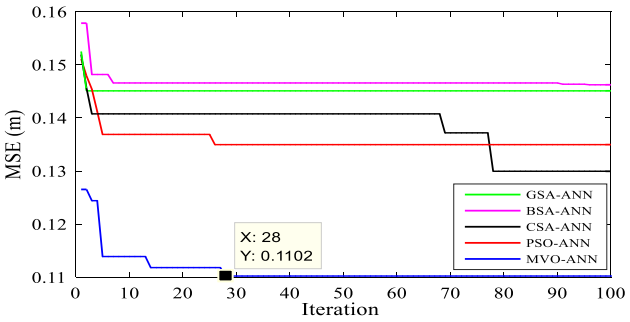

Fig. 10 The minimum standard error of the adopted soft-computing algorithms with respect to iteration

$$\text{Accuracy}_{\text{measu.}} = \left(1 - \frac{\text{measured} - \text{actual}}{\text{actual}}\right) \times 100\% \quad (6)$$

where measured denotes the measurement data recorded by the proposed SAS and *actual* indicates the measurement data recorded by the BM device.

8.2 Artificial neural network performance results

The data collected using the SAS were divided into training (70%), testing (15%), and validation (15%) of the performance of the MVO-ANN algorithm in terms of MSE and correlation coefficient (R^2). These performances are presented in Figs. 12 and 13.

In Fig. 12, the goal of the ANN was set to 1×10^{-3}, and the ANN stopped running either when the goal was accomplished or when it reached the optimal MSE. The ANN was able to reach its goal by increasing the number of epochs required to reach more than 2000 at the expense of increasing the ANN run-time to 200 s (compared to 12 s when 100 epochs were adopted). However, the results show that the adopted epochs yielded a satisfactory error and that there was no need to increase the epochs beyond 100, with Fig. 12 specifically showing that the number of epochs for MVO-ANN was set to 100 to evaluate the performance of the ANN and demonstrate that the network's performance did not reach the goal in terms of MSE

Table 2 The performance of five soft-computing algorithms hybridized with the ANN

Parameter	Algorithm				
	GSA-ANN	BSA-ANN	CSA-ANN	PSO-ANN	MVO-ANN
Learning rate	0.448	0.432	0.431	0.463	**0.751**
Neurons in first hidden layer	18	18	14	19	**20**
Neurons in Second hidden layer	17	11	12	14	**18**
No. of iterations	2	96	78	27	**28**
MSE	0.145	0.146	0.13	0.135	**0.110**

Bold parameters represent a better performance based on the MVO-ANN algorithm than other algorithms

Fig. 11 Architecture of the adopted artificial neural network

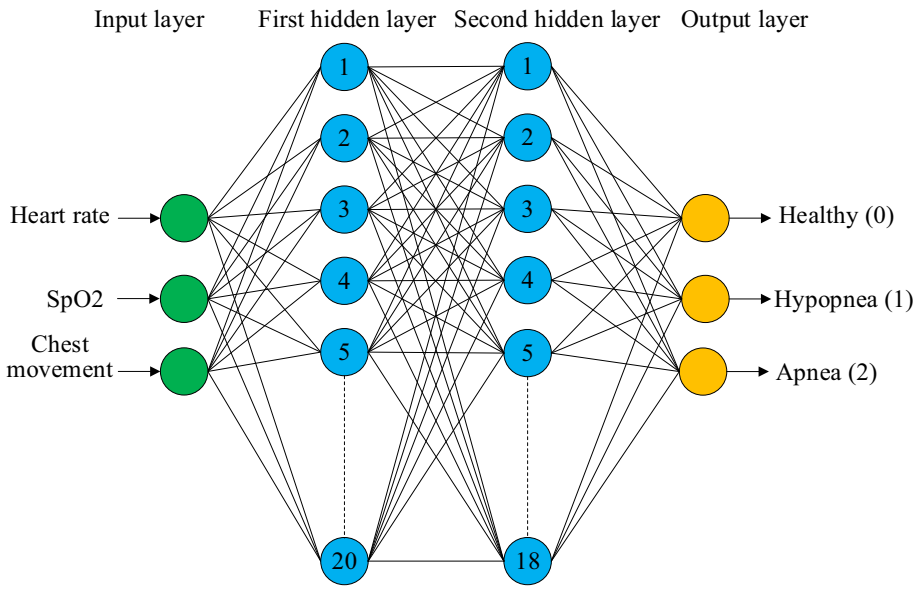

Content courtesy of Springer Nature, terms of use apply. Rights reserved.

Table 3 Adopted parameters of the artificial neural network

Parameters	Value	Note
Number of input layers	3	HR, SpO_2, and chest movement
Number of hidden layers	2	
Neurons in the first hidden layer	20	Obtained from MVO
Neurons in the second hidden layer	18	Obtained from MVO
Number of outputs	3	Healthy (0), Apnea (1), and Hypopnea (2)
Learning rate	0.75	Obtained based on MVO
Epochs	100	–
Target (goal)	1×10^{-3}	–
All collected data for each participant	25,200	Samples
Collected data for each sensor from each participant	8,400	Samples

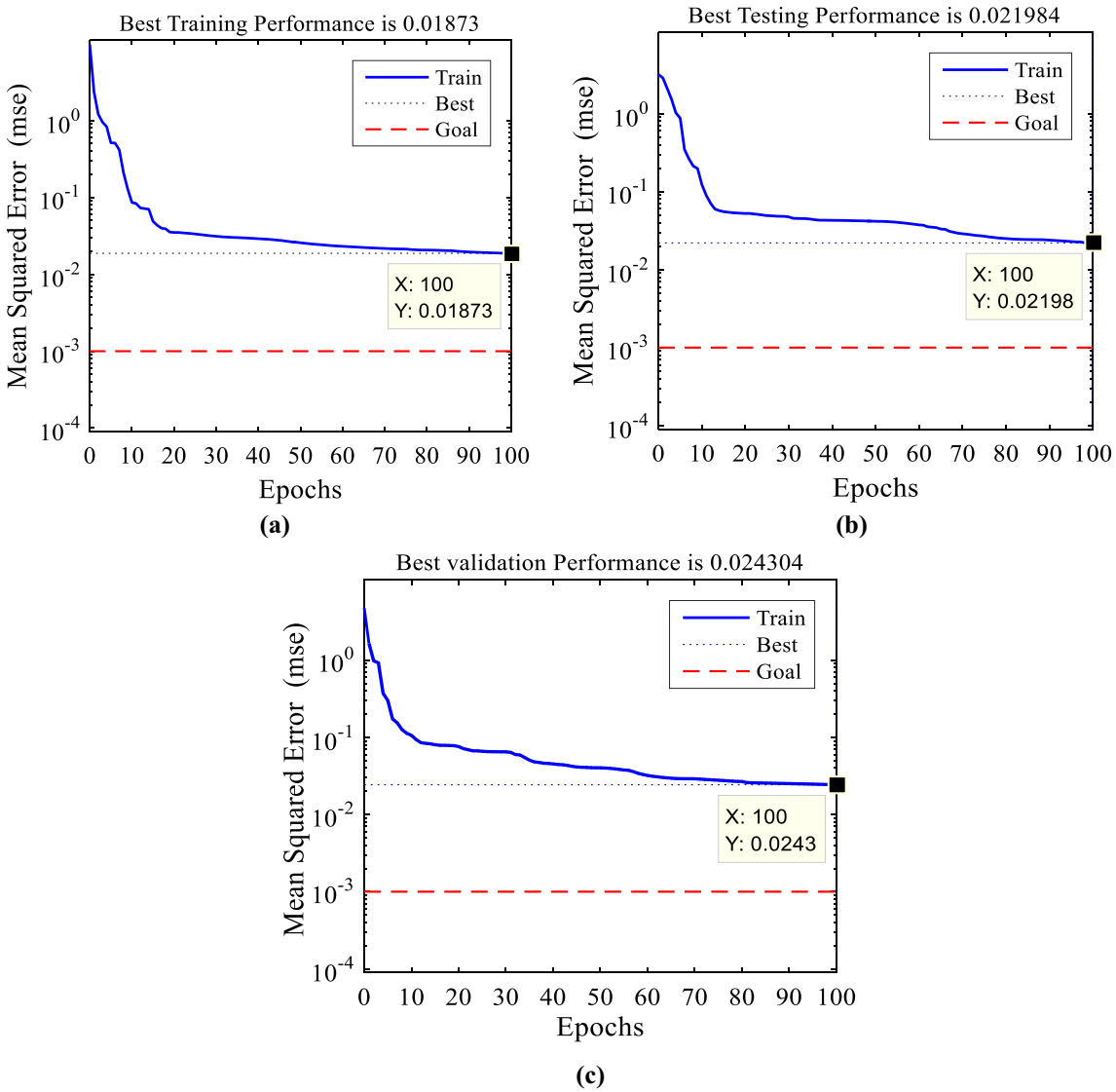

Fig. 12 The mean standard error of the multi-verse-optimizer–artificial-neural-network algorithm for **a** training, **b** testing, and **c** validation

Content courtesy of Springer Nature, terms of use apply. Rights reserved.

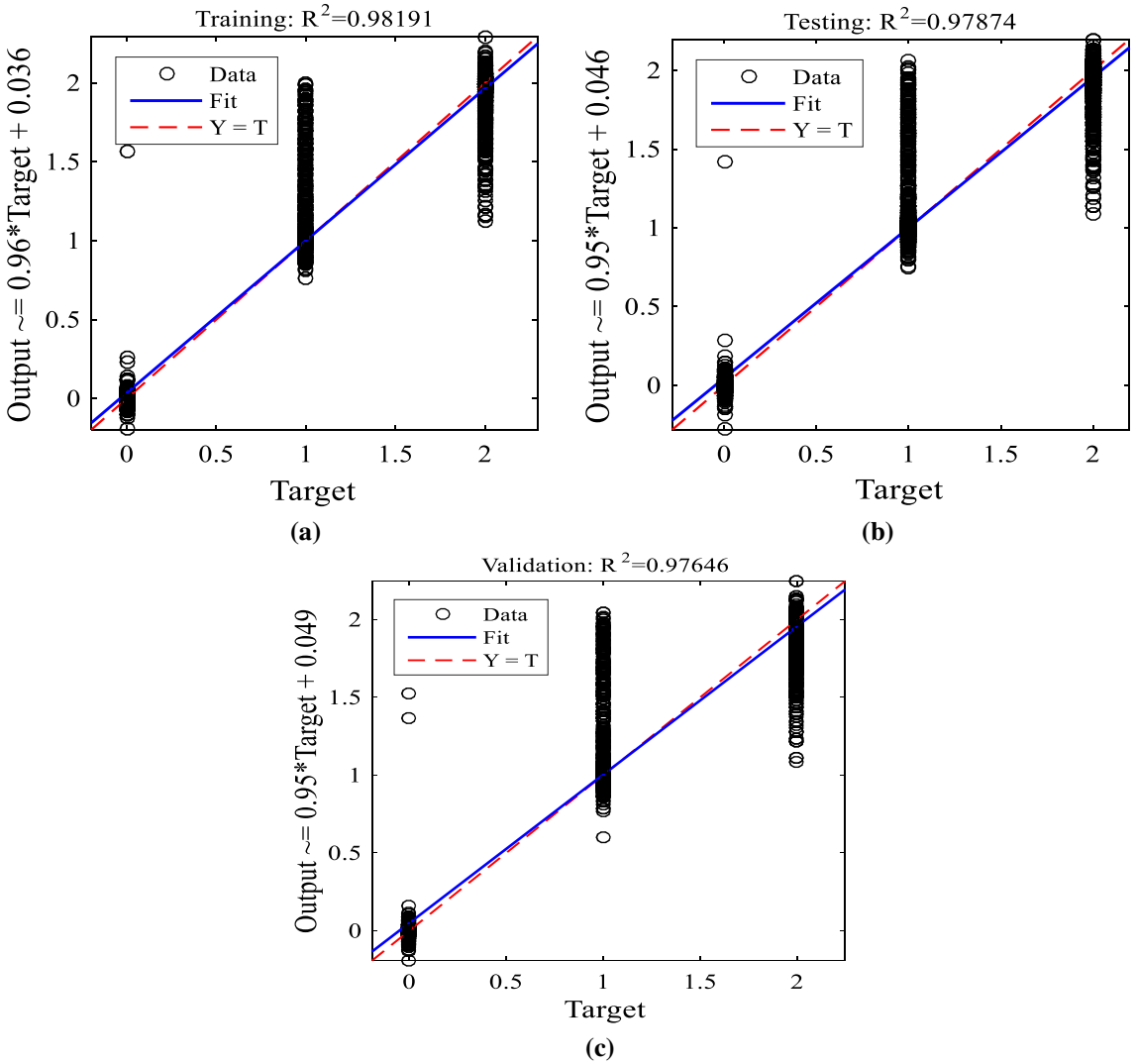

Fig. 13 The correlation coefficient of the multi-verse-optimizer–artificial-neural-network algorithm for **a** training, **b** testing, and **c** validation

(i.e., 1×10^{-3}) during either training, testing, or validation. The best MSE performance was found for 0.018 of training, 0.021 of testing, and 0.024 of validation, with Fig. 12a (training) demonstrating better results than those derived during testing and validation at 100 epochs and Fig. 12b (testing) indicating that the results obtained that were better than those obtained during validation. Nonetheless, 12c suggests convincing validation results.

The ANN's performance can also be investigated in terms of training, testing, and validation time, with processing time considered an important factor in real-time implementation. Training, validation, and testing times during the offline phase were 12 s, 9 s, and 8 s when the MVO-ANN was considered. In contrast, the corresponding times when MVO-ANN was not applied were 18 s, 17 s, and 13 s. One of the benefits of adopting the MVO-ANN is reducing the ANN's processing time during the offline phase by reducing the number of neurons in its hidden layers. This means that there is no need to be concerned about the time characteristic. Hence, following offline training of the ANN, the new sensor measurements are received by the MU. These correspond to real-time estimations of SA events.

Figure 13 presents the correlation coefficient of the ANN for training, testing, and validation. The correlation coefficient is a good indicator of the amount of agreement between the actual value and the estimated value. That is, it can demonstrate concordance between a patient's actual conditions (i.e., normal breathing, hypopnea, and apnea) and the values estimated by the MVO-ANN. The actual values were measured by plotting the proposed SAS on the x-axis (target) and plotting the estimated values obtained from the hybrid MVO-ANN on the y-axis (output). The ANN's output was denoted by the numbers "0" (normal or

Content courtesy of Springer Nature, terms of use apply. Rights reserved.

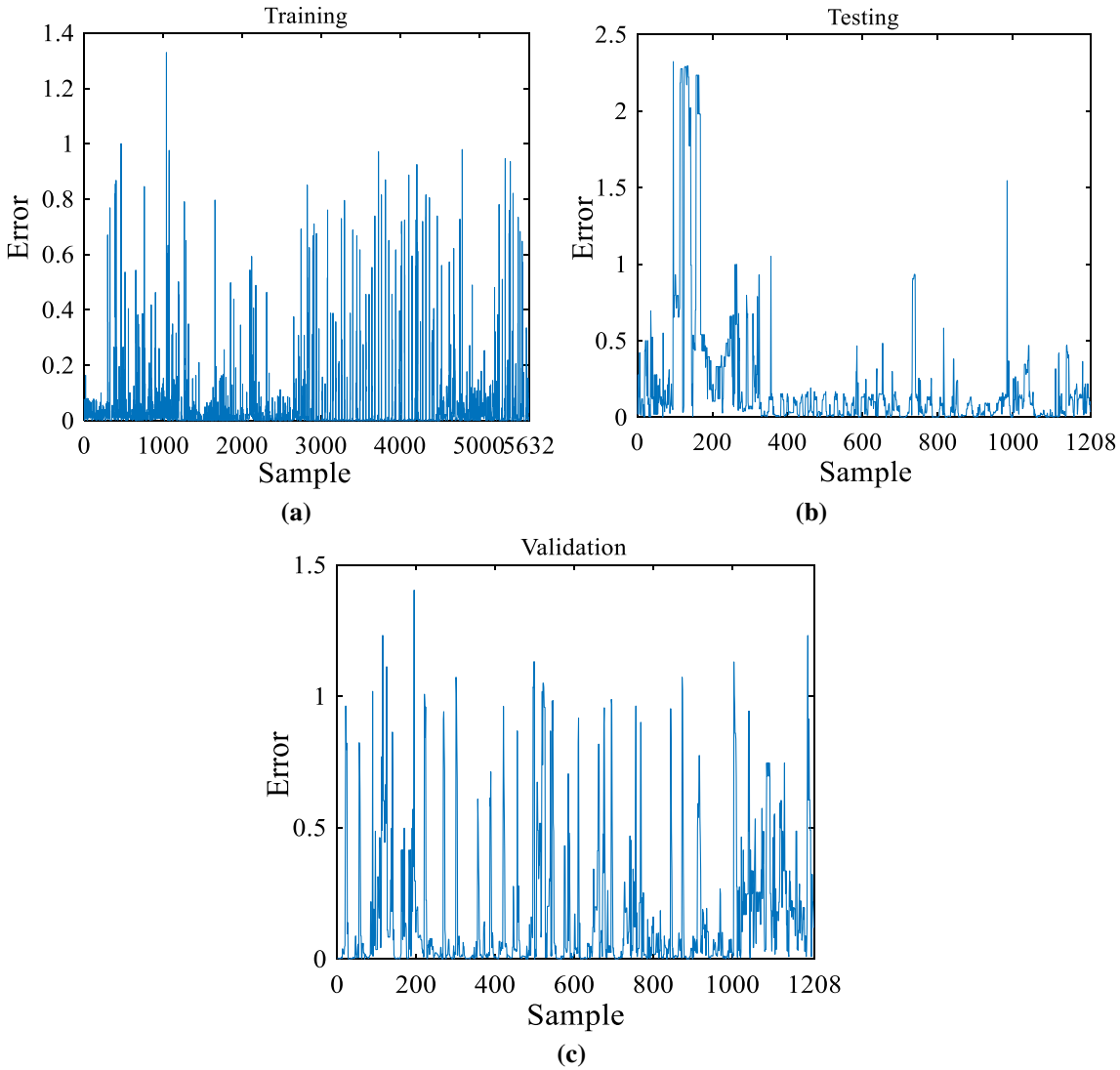

Fig. 14 Mean standard error of the multi-verse-optimizer–artificial-neural-network algorithm for **a** training, **b** testing, and **c** validation

Table 4 Error measurements of the multi-verse-optimizer–artificial-neural-network algorithm

Error	Training	Testing	Validation
MAE	0.042	0.202	0.166
MSE	0.014	0.202	0.093
RMSE	0.120	0.450	0.305

healthy breathing), "1" (hypopnea), and "2" (apnea). Figure 13a–c represent the correlation coefficients of the ANN: 0.981 for training, 0.978 for testing, and 0.976 for validation. These results presented in Fig. 13 provide strong evidence for the MVO-ANN algorithm's ability to accurately predict patient breathing conditions.

8.3 Error results

The MVO-ANN algorithm's performance was also measured according to error, as Fig. 14 illustrates. Figure 14a–c indicate more substantial errors in some positions relative to others, likely due to the movement of sensors while the patient was sleeping. Figure 14a suggests that the error rates obtained from the training set were lower than those obtained from the testing and validation sets, with the error ranging between 0 and 1.35. Figure 14b shows that the measured testing error varied between 0 and 2.25, while Fig. 14c demonstrates that errors during validation decreased, ranging between 0 and 1.4. Table 4 presents the MAE, MSE, and root MSE (RMSE) values of the ANN for training, testing, and validation.

Content courtesy of Springer Nature, terms of use apply. Rights reserved.

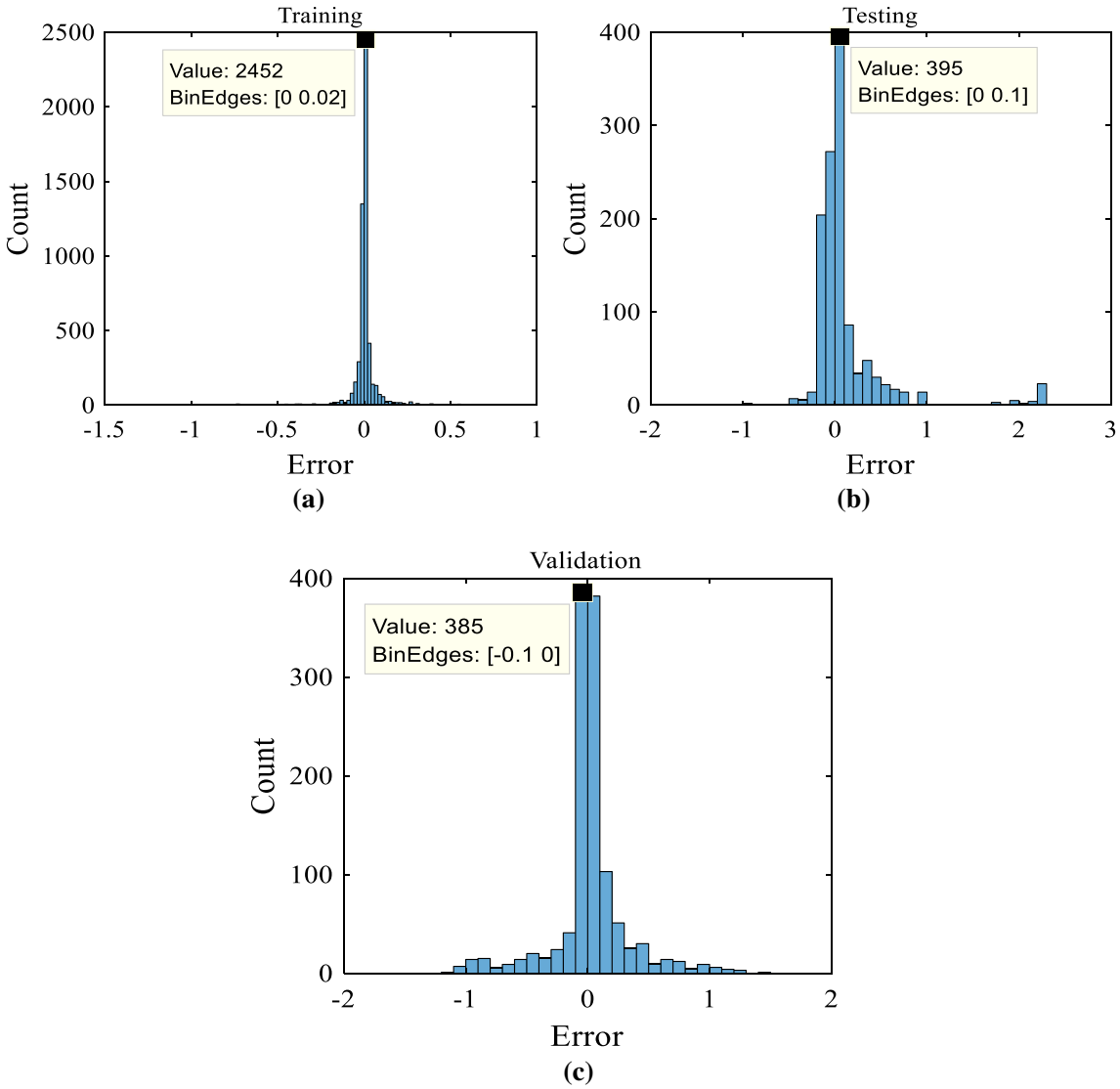

Fig. 15 Histogram of the multi-verse-optimizer–artificial-neural-network algorithm for **a** training, **b** testing, and **c** validation

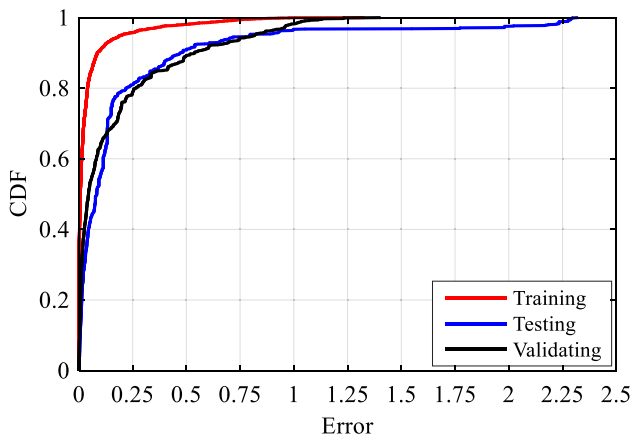

Fig. 16 The cumulative distribution function of the multi-verse-optimizer–artificial-neural-network algorithm

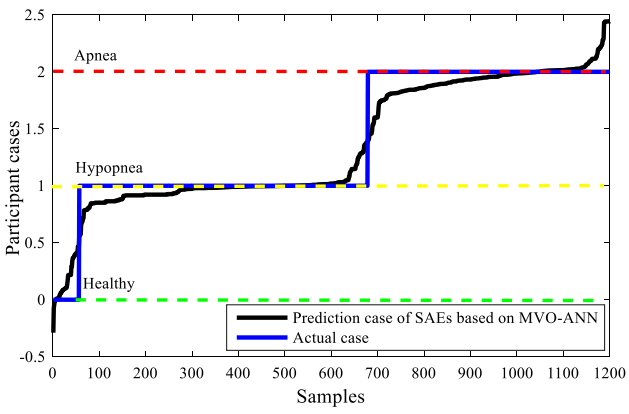

Fig. 17 Actual and predicted sleep apnea events

Content courtesy of Springer Nature, terms of use apply. Rights reserved.

Table 5 Comparison between previous research and current work

Ref./year	Method	ANN structure		No. of epoch	Performance metrics		
		HL	Neurons		SEN (%)	SPE (%)	ACC (%)
[33]/2019	DNN	N/M	N/M	N/M	93	**94**	93.1
	1D CNN				**99**	**99**	98.5
	2D CNN				**96**	**96**	95.9
	RNN				**97**	87	85.4
	LSTM				**98**	**98**	**98**
	GRU				**99**	**99**	**99**
[1]/2019	LM	10	32	N/M	N/M	N/M	N/M
[34]/2020	Combination of CNN, LSTM, and FCL	4	N/M	50	81	**87**	84
		128	128				
[36]/2013	LM	4	20	1000	N/M	N/M	**98.7**
	SCG	N/M	N/M	N/M	N/M	N/M	**96.7**
	BFGS	N/M	N/M	N/M	N/M	N/M	**96.3**
	OSS	N/M	N/M	N/M	N/M	N/M	**95.7**
	PBR	N/M	N/M	N/M	N/M	N/M	**96.3**
[37]/2019	SVM	N/M	N/M	N/M	**100**	98	99
	KNN	N/M	N/M	N/M	70	**92**	75
	ANN	N/M	N/M	N/M	75	**100**	86
[38]/2019	LR	N/M	N/M	N/M	72	**87.4**	81.5
	LDA				70.9	**88.4**	81.8
	SVM				72.1	**85.7**	80.6
	MLP				74.3	**85.7**	81.4
	TW-MLP				85.1	**88.7**	87.3
[3]/2019	DNN	10	30	10,000	N/M	N/M	**72.6**
[39]/2020	LSTM	N/M	N/M	N/M	58.4	**76.2**	72.8
[63]/2019	SVM	N/M	N/M	N/M	N/M	**98**	92.78
	KNN				N/M	**95**	92.18
[40]/2020	Feedforward	N/M	5	N/M	N/M	N/M	**85.14**
[41]/2020	Combination of CNN and LSTM	N/M	100	50	98.97	96.94	**99.80**
Current work	MVO-ANN	2	38	100	96.71	**99.24**	98.67

Bold performance metrics represent the maximum values of the state-of-the-art works and the current work

Ref: reference; *HL* hidden layer, *SEN* sensitivity, *SPE* specificity, *ACC* accuracy, *N/M* not mentioned

8.4 Histogram results

Figure 15 represents the amount of error associated with the MVO-ANN network in the form of histograms for the training, testing, and validation data. Outliers can be used to determine the quality of specific data, with Fig. 15a indicating that the training data's errors accumulated most at the zero point (2452) and Fig. 15b, c indicating that the testing and validation data also featured considerable accumulation (395 and 385) at the zero point, with limited errors outside of points near zero, with the validation data producing only a very small amount of errors between − 1 and 1.

8.5 Cumulative distribution function plot results

The cumulative distribution function is presented in Fig. 16. It investigates the ANN's measure of error, with the red curve referring to training, the blue curve referring to testing (featuring a greater degree of error), and the black curve referring to validation. The training curve demonstrably features the smallest error. The training error was 1.32, the testing error was 1.4, and the validation error was 2.32. Figure 16 demonstrates that 95% of the prediction error associated with the training curve was below 0.19. Meanwhile, 95% of the prediction error for the testing curve was below 0.8, and 95% of the prediction error for

Content courtesy of Springer Nature, terms of use apply. Rights reserved.

the validation curve was below 0.81. Thus, Fig. 16 indicates that the probability of detecting respiratory events was comparable for testing and validating at the 95% level.

8.6 Predicting sleep apnea events

As Sect. 7 indicated, the output of the MOV-ANN indicates one of three cases, which are denoted by "0" (normal or healthy breathing), "1" (hypopnea), and "2" (apnea). A healthy case indicates that the participant does not suffer from sleep apnea. The apnea case indicates that the patient has SA. However, hypopnea indicates a condition that is less severe than SA. This means that the hypopnea case can be utilized to predict SA before it happens. Figure 17 shows the correlation between SAEs predicted by the MVO-ANN (the black line) and the actual cases indicated during the validation process (healthy, hypopnea, and apnea as a blue line). The figure also specifically indicates the three distinct cases identified by the ANN's output: healthy (green line), hypopnea (yellow line), and apnea (red line), revealing that the predictions draw level with the pattern of actual cases alongside the samples, indicating a good fit based on the scale of the plot. That is, Fig. 17 reveals close agreement between prediction and actual cases in terms of validating the ANN.

9 Sleep apnea system performance evaluation

The SAS's performance—in terms of detecting and predicting SAEs—was evaluated using a statistical analysis that considered accuracy, sensitivity, and specificity. These statistical markers were selected to measure the reliability of the proposed SAS in relation to the methods and results of previous studies. Accuracy, sensitivity, and specificity were measured according to the following equations:

$$\text{accuracy} = \frac{(TP + TN)}{(FP + TN + TP + FN)} \times 100\% \quad (7)$$

$$\text{specificity} = \frac{TN}{(TN + FP)} \times 100\% \quad (8)$$

$$\text{sensitivity} = \frac{TP}{(TP + FN)} \times 100\% \quad (9)$$

where TP denotes true positive (the number of normal events that are recorded as normal), TN denotes true negative (the number of abnormal events that are recorded as abnormal), FP denotes false positive (the number of abnormal events that are recorded as normal), and FN denotes false negative (the number of normal events recorded as abnormal).

Applying Eqs. (7), (8), and (9) to the proposed SAS revealed an accuracy of 98.67%, a sensitivity of 96.71%, and a specificity of 99.24%.

10 Comparison with the results of previous research

This section compares the performance of the proposed SAS with the results presented in previous research concerning adopted algorithms, numbers of hidden layers, neurons, numbers of participants, sensitivity, specificity, and accuracy (see Table 5). Most of the results presented in this paper were comparable to or outperformed the findings reported by previous studies, likely because those previous papers considered artificial techniques. Notably, the SAS performed slightly better than other approaches in terms of specificity. Measurement accuracy is a key factor in the design of a medical device, and, promisingly, the proposed SAS achieved a relatively high accuracy of 98.67%, outperforming most of the existing methods considered. The proposed SAS also features several benefits in comparison to other approaches. Not only does it adopt low-power sensors (pulse oximeter and flex), it is small and lightweight, easy to set up, and inexpensive, adopting BLE wireless communication allows rapid diagnosis and free movement during sleep, and the low-power components mean that the SAS is capable of long-term monitoring. Although a trade-off between measurement accuracy and the benefits provided by the proposed SAS was necessary, the device's accuracy can be improved to approach the BM (i.e., HSAT). However, this might come at the expense of increasing the system's cost and complexity as a result of adding other sensors, such as oronasal airflow sensors, position sensors, EEG, or ECG. Future research could consider such modifications.

11 Conclusions

The current research involved collecting data using a new SAS featuring three sensors: HR, SpO_2, and flex. These parameters were measured and transmitted from the patient's body to the MU via BLE 4.0 to predict the frequency and severity of SAEs. The measurements were comfortable for the sleeping patients because they could move freely. A total of 25,200 data samples were gathered from 10 volunteers, six of whom were suffering from SA and four of whom were healthy. The data collected from the patients for the three sensors were used to train (70%), test (15%), and validate (15%) the ANN. Five hybrid algorithms (GSA-ANN, BSA-ANN, CSA-ANN, PSO-ANN, and MVO-ANN) were considered to determine

Content courtesy of Springer Nature, terms of use apply. Rights reserved.

which featured the best hidden-layer neuron count and which featured a learning rate producing the lowest MSE. Identifying such an algorithm aimed to enable accurate prediction of respiratory events before they happen, and the results indicated that the MVO-ANN algorithm performed better in terms of error (MSE = 0.11).

Slight errors in the results were probably due to the movement of the pulse oximeter sensor that was attached to the patient's finger, movement of which can promote sudden changes in HR or SpO_2 readings. Nonetheless, the results obtained for the proposed SAS indicate that it can reliably predict respiratory events, with the experimental results suggesting the device achieved 98.67% accuracy, 96.71% sensitivity, and 99.24% specificity.

From a technical perspective, future research should seek to use other algorithms to reduce error and increase the degree of correspondence between real and predicted respiratory events. Using certain strategies for reducing the energy consumption of the SAS and increasing its battery life is critical to increasing patient monitoring time, which was only 17 h in the current study. In terms of treatment, positive airway pressure (PAP) devices are among the best non-surgical treatments for people suffering from SA. These devices provide continuous positive pressure to open the airway and prevent it from blocking. However, using the device continuously can produce various side effects, including congestion, dryness, sneezing, runny nose, sore throat, and irritated eyes. Given that the proposed SAS can predict respiratory events before they occur, it could be used to develop a device that can control the PAP device. Designing this type of "smart" PAP device would reduce the side effects associated with using such devices.

Acknowledgements The author would like to thank the staff of the Department of Medical Instrumentation Techniques Engineering, Electrical Engineering Technical College, Middle Technical University, and Al-Kafeel Super Specialty Hospital in Karbala for their support during this study.

Declarations

Conflict of interest All authors certify that they have no affiliations with or involvement in any organization or entity with any financial interest or non-financial interest in the subject matter or materials discussed in this manuscript. The authors did not receive support from any organization to complete the submitted work. None of the authors received payment or services from a third party for any aspect of the submitted work at any time (including but not limited to grants or assistance at, e.g., the data monitoring, study design, manuscript preparation or statistical analysis stage).

Human and animal rights The research involved human participants. The participant information sheet and consent forms are attached at the end of this manuscript.

References

1. Ferduła R, Walczak T, Cofta S (2019) The application of artificial neural network in diagnosis of sleep apnea syndrome. In: Advances in manufacturing II. Springer, pp 432–443
2. Thorey V, Hernandez AB, Arnal PJ (2019) During EH AI vs humans for the diagnosis of sleep apnea. In: 41st annual international conference of the IEEE engineering in medicine and biology society (EMBC), Berlin, Germany, Germany, 23–27. pp 1596–1600. https://doi.org/10.1109/EMBC.2019.8856877
3. De Falco I, De Pietro G, Della Cioppa A, Sannino G, Scafuri U, Tarantino E (2019) Evolution-based configuration optimization of a deep neural network for the classification of obstructive sleep apnea episodes. Future Gener Comput Syst 98:377–391. https://doi.org/10.1016/j.future.2019.01.049
4. Dong Z, Xu X, Wang C, Cartledge S, Maddison R, Islam SMS (2020) Association of overweight and obesity with obstructive sleep apnoea: a systematic review and meta-analysis. Obes Med 17:100185
5. Chyad MH, Gharghan SK, Hamood HQ (2020) A survey on detection and prediction methods for sleep apnea. IOP Conf Ser: Mater Sci Eng 1:012102
6. Badr MS, Javaheri S (2019) Central sleep apnea: a brief review. Curr Pulmonol Rep 8(1):14–21
7. Collen J, Lettieri C, Wickwire E, Holley A (2020) Obstructive sleep apnea and cardiovascular disease, a story of confounders! Sleep Breath 1–15
8. Yao X, Li M, Yao L, Shao L (2020) Obstructive sleep apnea and hypertension. In: Secondary hypertension. Springer, pp 461–488
9. Qie R, Zhang D, Liu L, Ren Y, Zhao Y, Liu D, Liu F, Chen X, Cheng C, Guo C (2020) Obstructive sleep apnea and risk of type 2 diabetes mellitus: a systematic review and dose-response meta-analysis of cohort studies. J Diabetes 12(6):455–464
10. Ruchała M, Bromińska B, Cyrańska-Chyrek E, Kuźnar-Kamińska B, Kostrzewska M, Batura-Gabryel H (2017) Obstructive sleep apnea and hormones–a novel insight. Arch Med Sci 13(4):875
11. Kamble PG, Theorell-Haglöw J, Wiklund U, Franklin KA, Hammar U, Lindberg E, Eriksson JW (2020) Sleep apnea in men is associated with altered lipid metabolism, glucose tolerance, insulin sensitivity, and body fat percentage. Endocrine 1–10
12. Zhou J, Wu X-m, Zeng W-j (2015) Automatic detection of sleep apnea based on EEG detrended fluctuation analysis and support vector machine. J Clin Monit Comput 29(6):767–772
13. Almendros I, Martinez-Garcia MA, Farré R, Gozal D (2020) Obesity, sleep apnea, and cancer. Int J Obes 44:1653–1667
14. McNab AA (2007) The eye and sleep apnea. Sleep Med Rev 11(4):269–276
15. Mendonça F, Mostafa SS, Morgado-Dias F, Navarro-Mesa JL, Juliá-Serdá G, Ravelo-García AG (2018) A portable wireless device based on oximetry for sleep apnea detection. Computing 100(11):1203–1219
16. Haidar R, Koprinska I, Jeffries B (2017) Sleep apnea event detection from nasal airflow using convolutional neural networks. In: International conference on neural information processing, Guangzhou, China, 14–18. Springer, pp 819–827
17. Mendonca F, Mostafa SS, Ravelo-García AG, Morgado-Dias F, Penzel T (2018) A review of obstructive sleep apnea detection approaches. IEEE J Biomed Health Inform 23(2):825–837
18. Haoyu L, Jianxing L, Arunkumar N, Hussein AF, Jaber MM (2019) An IoMT cloud-based real time sleep apnea detection scheme by using the SpO2 estimation supported by heart rate variability. Future Gener Comput Syst 98:69–77
19. Hang L-W, Wang H-L, Chen J-H, Hsu J-C, Lin H-H, Chung W-S, Chen Y-F (2015) Validation of overnight oximetry to

Content courtesy of Springer Nature, terms of use apply. Rights reserved.

diagnose patients with moderate to severe obstructive sleep apnea. BMC Pulm Med 15(1):24
20. Gutiérrez-Tobal GC, Kheirandish-Gozal L, Álvarez D, Crespo A, Philby MF, Mohammadi M, del Campo F, Gozal D, Hornero R (2015) Analysis and classification of oximetry recordings to predict obstructive sleep apnea severity in children. In: 37th annual international conference of the IEEE engineering in medicine and biology society (EMBC), Milan, Italy, 25–29. IEEE, pp 4540–4543
21. Sánchez-Morillo D, López-Gordo M, León A (2014) Novel multiclass classification for home-based diagnosis of sleep apnea hypopnea syndrome. Expert Syst Appl 41(4):1654–1662
22. Marcos JV, Hornero R, Alvarez D, Aboy M, Del Campo F (2011) Automated prediction of the apnea-hypopnea index from nocturnal oximetry recordings. IEEE Trans Biomed Eng 59(1):141–149
23. Oliver N, Flores-Mangas F (2007) Healthgear: Automatic sleep apnea detection and monitoring with a mobile phone. J Commun 2(2):1–9
24. Chesson AL Jr, Berry RB, Pack A (2003) Practice parameters for the use of portable monitoring devices in the investigation of suspected obstructive sleep apnea in adults. Sleep 26(7):907–913
25. Kalkbrenner C, Eichenlaub M, Rüdiger S, Kropf-Sanchen C, Rottbauer W, Brucher R (2018) Apnea and heart rate detection from tracheal body sounds for the diagnosis of sleep-related breathing disorders. Med Biol Eng Comput 56(4):671–681
26. Yadollahi A, Giannouli E, Moussavi Z (2010) Sleep apnea monitoring and diagnosis based on pulse oximetery and tracheal sound signals. Med Biol Eng Comput 48(11):1087–1097
27. Chen L, Zhang X, Wang H (2015) An obstructive sleep apnea detection approach using kernel density classification based on single-lead electrocardiogram. J Med Syst 39(5):47
28. Almuhammadi WS, Aboalayon KA, Faezipour M (2015) Efficient obstructive sleep apnea classification based on EEG signals. In: Long Island systems, applications and technology, Farmingdale, NY, USA, 1–1. IEEE, pp 1–6
29. Malaekah E, Patti CR, Cvetkovic D (2014) Automatic sleep-wake detection using electrooculogram signals. In: IEEE conference on biomedical engineering and sciences (IECBES), Kuala Lumpur, Malaysia, 8–10. IEEE, pp 724–728
30. Kopaczka M, Oezkan O, Merhof D (2017) Face tracking and respiratory signal analysis for the detection of sleep apnea in thermal infrared videos with head movement. In: International conference on image analysis and processing, Catania-Italy, 11–15. Springer, pp 163–170
31. Hung PD (2018) Central sleep apnea detection using an accelerometer. In: International conference on control and computer vision, Singapore, Singapore 15–18. ACM, pp 106–111
32. Gharghan SK, Nordin R, Ismail M, Ali JA (2015) Accurate wireless sensor localization technique based on hybrid PSO-ANN algorithm for indoor and outdoor track cycling. IEEE Sens J 16(2):529–541
33. Erdenebayar U, Kim YJ, Park J-U, Joo EY, Lee K-J (2019) Deep learning approaches for automatic detection of sleep apnea events from an electrocardiogram. Comput Methods Programs Biomed 180:105001. https://doi.org/10.1016/j.cmpb.2019.105001
34. Hafezi M, Montazeri N, Saha S, Zhu K, Gavrilovic B, Yadollahi A, Taati B (2020) Sleep apnea severity estimation from tracheal movements using a deep learning model. IEEE Access 8:22641–22649
35. Mahmud T, Khan IA, Mahmud TI, Fattah SA, Zhu W-P, Ahmad MO (2020) Sleep apnea event detection from sub-frame based feature variation in EEG signal using deep convolutional neural network. In: 42nd Annual international conference of the IEEE engineering in medicine & biology society (EMBC), Montreal, QC, Canada, 20–24. IEEE, pp 5580–5583
36. Sankar AB, Selvi JAV, Kumar D, Lakshmi KS (2013) Effective enhancement of classification of respiratory states using feed forward back propagation neural networks. Sadhana 38(3):377–395
37. Vimala V, Ramar K, Ettappan M (2019) An intelligent sleep apnea classification system based on EEG signals. J Med Syst 43(2):36
38. Wang T, Lu C, Shen G (2019) Detection of sleep apnea from single-lead ECG signal using a time window artificial neural network. Biomed Res Int. https://doi.org/10.1155/2019/9768072
39. Van Steenkiste T, Groenendaal W, Dreesen P, Lee S, Klerkx S, De Francisco R, Deschrijver D, Dhaene T (2020) Portable detection of apnea and hypopnea events using bio-impedance of the chest and deep learning. IEEE J Biomed Health Inform 24(9):2589–2598
40. Hassan O, Parvin D, Kamrul S (2020) Machine learning model based digital hardware system design for detection of sleep apnea among neonatal infants. In: 63rd international midwest symposium on circuits and systems (MWSCAS), Springfield, MA, USA, 9–12. IEEE, pp 607–610
41. Liang X, Qiao X, Li Y (2019) Obstructive sleep apnea detection using combination of CNN and LSTM techniques. In: 8th Joint international information technology and artificial intelligence conference (ITAIC), Chongqing, China, 24–26. IEEE, pp 1733–1736
42. Toften S, Kjellstadli JT, Tyvold SS, Moxness MHS (2021) A pilot study of detecting individual sleep apnea events using noncontact radar technology, pulse oximetry, and machine learning. J Sens 2021:2998202. https://doi.org/10.1155/2021/2998202
43. Alvarez D, Hornero R, Marcos JV, del Campo F (2010) Multivariate analysis of blood oxygen saturation recordings in obstructive sleep apnea diagnosis. IEEE Trans Biomed Eng 57(12):2816–2824
44. Lin SH, Branson C, Park L, Leung J, Doshi N, Auerbach SH (2018) Oximetry as an accurate tool for identifying moderate to severe sleep apnea in patients with acute stroke. J Clin Sleep Med 14(12):2065–2073
45. Nigro CA, Dibur E, Rhodius E (2011) Pulse oximetry for the detection of obstructive sleep apnea syndrome: can the memory capacity of oxygen saturation influence their diagnostic accuracy? Sleep Disorders 2011:427028. https://doi.org/10.1155/2011/427028
46. Garde A, Dehkordi P, Wensley D, Ansermino JM, Dumont GA (2015) Pulse oximetry recorded from the Phone Oximeter for detection of obstructive sleep apnea events with and without oxygen desaturation in children. In: 2015 37th annual international conference of the IEEE engineering in medicine and biology society (EMBC), MiCo - Milano Conference Center - Milan, Italy, August 25–29. IEEE, pp 7692–7695
47. Zubaidi SL, Ortega-Martorell S, Al-Bugharbee H, Olier I, Hashim KS, Gharghan SK, Kot P, Al-Khaddar R (2020) Urban water demand prediction for a city that suffers from climate change and population growth: Gauteng province case study. Water 12(7):1885
48. Zubaidi SL, Abdulkareem IH, Hashim KS, Al-Bugharbee H, Ridha HM, Gharghan SK, Al-Qaim FF, Muradov M, Kot P, Al-Khaddar R (2020) Hybridised artificial neural network model with slime mould algorithm: a novel methodology for prediction of urban stochastic water demand. Water 12(10):2692
49. Munadhil Z, Gharghan SK, Mutlag AH, Al-Naji A, Chahl J (2020) Neural network-based Alzheimer's patient localization for wireless sensor network in an indoor environment. IEEE Access 8:150527–150538
50. Gohari M, Rahman RA, Raja RI, Tahmasebi M (2012) A novel artificial neural network biodynamic model for prediction seated

Content courtesy of Springer Nature, terms of use apply. Rights reserved.

human body head acceleration in vertical direction. J Low Freq Noise Vib Act Control 31(3):205–216
51. Gohari M, Rahman R, Tahmasebi M, Nejat P (2014) Off-road vehicle seat suspension optimisation, part I: derivation of an artificial neural network model to predict seated human spine acceleration in vertical vibration. J Low Freq Noise Vib Act Control 33(4):429–441
52. Henríquez PA, Ruz GA (2018) A non-iterative method for pruning hidden neurons in neural networks with random weights. Appl Soft Comput 70:1109–1121
53. Motahar S, Jahangiri M (2020) Transient heat transfer analysis of a phase change material heat sink using experimental data and artificial neural network. Appl Therm Eng 167:114817
54. Ang ZH, Ang CK, Lim WH, Yu LJ, Solihin MI (2020) Development of an artificial intelligent approach in adapting the characteristic of polynomial trajectory planning for robot manipulator. Int J Mech Eng Robot Res 9(3):408–414
55. Mahdi SQ, Gharghan SK, Hasan MA (2021) FPGA-Based neural network for accurate distance estimation of elderly falls using WSN in an indoor environment. Measurement 167:108276
56. Kapanova KG, Dimov I, Sellier JM (2018) A genetic approach to automatic neural network architecture optimization. Neural Comput Appl 29(5):1481–1492. https://doi.org/10.1007/s00521-016-2510-6
57. Alemu HZ, Wu W, Zhao J (2018) Feedforward neural networks with a hidden layer regularization method. Symmetry 10(10):525
58. Zubaidi SL, Hashim K, Ethaib S, Al-Bdairi NSS, Al-Bugharbee H, Gharghan SK (2020) A novel methodology to predict monthly municipal water demand based on weather variables scenario. J King Saud Univ-Eng Sci. https://doi.org/10.1016/j.jksues.2020.09.011
59. Mirjalili S, Mirjalili SM, Hatamlou A (2016) Multi-verse optimizer: a nature-inspired algorithm for global optimization. Neural Comput Appl 27(2):495–513
60. Fathy A, Rezk H (2018) Multi-verse optimizer for identifying the optimal parameters of PEMFC model. Energy 143:634–644. https://doi.org/10.1016/j.energy.2017.11.014
61. Shukri SE, Al-Sayyed R, Hudaib A, Mirjalili S (2021) Enhanced multi-verse optimizer for task scheduling in cloud computing environments. Expert Syst Appl 168:114230. https://doi.org/10.1016/j.eswa.2020.114230
62. Tabrizchi H, Tabrizchi M, Tabrizchi H (2020) Breast cancer diagnosis using a multi-verse optimizer-based gradient boosting decision tree. SN Appl Sci 2(4):752. https://doi.org/10.1007/s42452-020-2575-9
63. Tuncer SA, Akılotu B, Toraman S (2019) A deep learning-based decision support system for diagnosis of OSAS using PTT signals. Med Hypotheses 127:15–22

Publisher's Note Springer Nature remains neutral with regard to jurisdictional claims in published maps and institutional affiliations.

Content courtesy of Springer Nature, terms of use apply. Rights reserved.

Terms and Conditions

Springer Nature journal content, brought to you courtesy of Springer Nature Customer Service Center GmbH (“Springer Nature”).
Springer Nature supports a reasonable amount of sharing of research papers by authors, subscribers and authorised users (“Users”), for small-scale personal, non-commercial use provided that all copyright, trade and service marks and other proprietary notices are maintained. By accessing, sharing, receiving or otherwise using the Springer Nature journal content you agree to these terms of use (“Terms”). For these purposes, Springer Nature considers academic use (by researchers and students) to be non-commercial.
These Terms are supplementary and will apply in addition to any applicable website terms and conditions, a relevant site licence or a personal subscription. These Terms will prevail over any conflict or ambiguity with regards to the relevant terms, a site licence or a personal subscription (to the extent of the conflict or ambiguity only). For Creative Commons-licensed articles, the terms of the Creative Commons license used will apply.
We collect and use personal data to provide access to the Springer Nature journal content. We may also use these personal data internally within ResearchGate and Springer Nature and as agreed share it, in an anonymised way, for purposes of tracking, analysis and reporting. We will not otherwise disclose your personal data outside the ResearchGate or the Springer Nature group of companies unless we have your permission as detailed in the Privacy Policy.
While Users may use the Springer Nature journal content for small scale, personal non-commercial use, it is important to note that Users may not:

1. use such content for the purpose of providing other users with access on a regular or large scale basis or as a means to circumvent access control;
2. use such content where to do so would be considered a criminal or statutory offence in any jurisdiction, or gives rise to civil liability, or is otherwise unlawful;
3. falsely or misleadingly imply or suggest endorsement, approval , sponsorship, or association unless explicitly agreed to by Springer Nature in writing;
4. use bots or other automated methods to access the content or redirect messages
5. override any security feature or exclusionary protocol; or
6. share the content in order to create substitute for Springer Nature products or services or a systematic database of Springer Nature journal content.

In line with the restriction against commercial use, Springer Nature does not permit the creation of a product or service that creates revenue, royalties, rent or income from our content or its inclusion as part of a paid for service or for other commercial gain. Springer Nature journal content cannot be used for inter-library loans and librarians may not upload Springer Nature journal content on a large scale into their, or any other, institutional repository.
These terms of use are reviewed regularly and may be amended at any time. Springer Nature is not obligated to publish any information or content on this website and may remove it or features or functionality at our sole discretion, at any time with or without notice. Springer Nature may revoke this licence to you at any time and remove access to any copies of the Springer Nature journal content which have been saved.
To the fullest extent permitted by law, Springer Nature makes no warranties, representations or guarantees to Users, either express or implied with respect to the Springer nature journal content and all parties disclaim and waive any implied warranties or warranties imposed by law, including merchantability or fitness for any particular purpose.
Please note that these rights do not automatically extend to content, data or other material published by Springer Nature that may be licensed from third parties.
If you would like to use or distribute our Springer Nature journal content to a wider audience or on a regular basis or in any other manner not expressly permitted by these Terms, please contact Springer Nature at

onlineservice@springernature.com

View publication stats